

Energy & Environmental Science

Accepted Manuscript



This is an *Accepted Manuscript*, which has been through the Royal Society of Chemistry peer review process and has been accepted for publication.

Accepted Manuscripts are published online shortly after acceptance, before technical editing, formatting and proof reading. Using this free service, authors can make their results available to the community, in citable form, before we publish the edited article. We will replace this *Accepted Manuscript* with the edited and formatted *Advance Article* as soon as it is available.

You can find more information about *Accepted Manuscripts* in the [Information for Authors](#).

Please note that technical editing may introduce minor changes to the text and/or graphics, which may alter content. The journal's standard [Terms & Conditions](#) and the [Ethical guidelines](#) still apply. In no event shall the Royal Society of Chemistry be held responsible for any errors or omissions in this *Accepted Manuscript* or any consequences arising from the use of any information it contains.

**Electrochemical Oxidation of H₂ Catalyzed by Ruthenium Hydride Complexes
Bearing P₂N₂ Ligands With Pendant Amines as Proton Relays**

Tianbiao Liu,* Mary Rakowski DuBois, Daniel L. DuBois and R. Morris Bullock*

Center for Molecular Electrocatalysis, Physical Sciences Division, Pacific Northwest National
Laboratory, P.O. Box 999, K2-57, Richland, WA 99352

morris.bullock@pnnl.gov, tianbiao.liu@pnnl.gov

Abstract: Two Ru hydride complexes, Cp*Ru(P^{Ph}₂N^{Bn}₂)H (**1-H**) and Cp*Ru(P^{tBu}₂N^{Bn}₂)H (**2-H**) supported by cyclic P^R₂N^{R'}₂ ligands (Cp* = η⁵-C₅Me₅; 1,5-dibenzyl,-3,7-R-1,5-diaza-3,7-diphosphacyclooctane, where R = Ph or ^tBu) have been developed as electrocatalysts for oxidation of H₂ (1.0 atm, 22 °C). The turnover frequency of **2-H** is 1.2 s⁻¹ at 22 °C (1.0 atm H₂) with an overpotential at E_{cat/2} of 0.5 V in the presence of exogenous base, DBU (1,8-diazabicyclo[5.4.0]undec-7-ene), while catalysis by **1-H** has a turnover frequency of 0.6 s⁻¹ and an overpotential of 0.6 V at E_{cat/2}. Addition of H₂O facilitates oxidation of H₂ by **2-H** and increases its turnover frequency to 1.9 s⁻¹, while H₂O slows down the catalysis by **1-H**. In addition, studies of Cp*Ru(dmpm)H (where dmpm = bis(dimethylphosphino)methane), a control complex lacking pendant amines in its diphosphine ligand, confirms the critical roles of the pendant amines of the P₂N₂ ligands as proton relays in the oxidation of H₂.

Broader context

Substantial progress has been achieved in recent years on the development of molecular electrocatalysts for the production of hydrogen by reduction of protons, but far fewer catalysts are known for the opposite reaction, oxidation of hydrogen. The oxidation of hydrogen provides

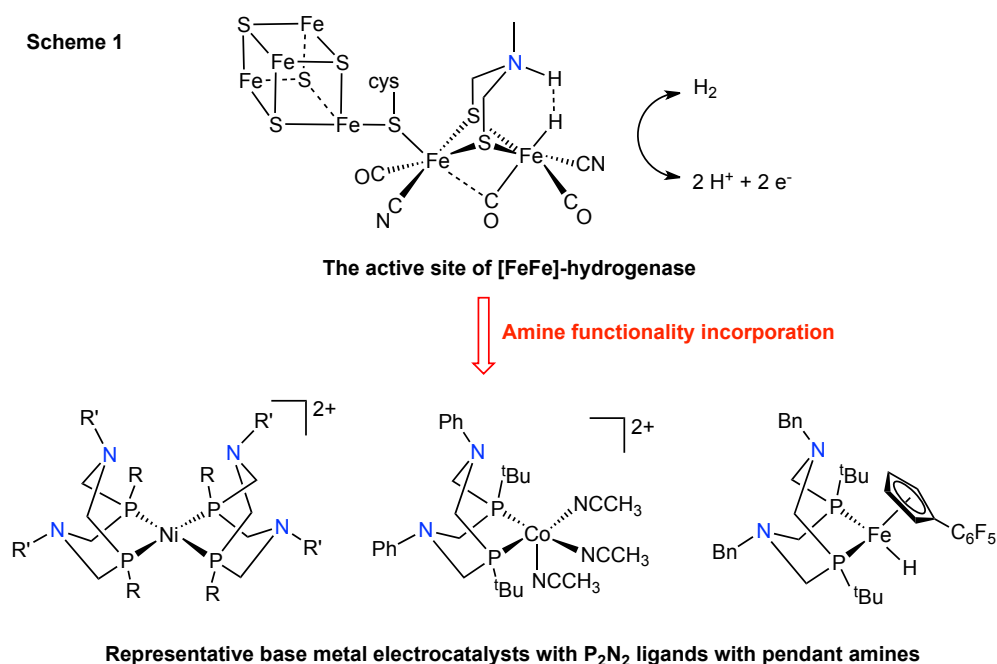
a means of converting the chemical energy of the H-H bond into electrical power in PEM fuel cells, but is typically catalyzed by platinum based catalysts. Hydrogenase enzymes in nature catalyze both the production and oxidation of hydrogen, and a key functionality in the [FeFe] hydrogenases is an amine base that functions as a proton relay. We report in this paper the synthesis and characterization of two molecular ruthenium hydride complexes that are a new class of molecular electrocatalysts for the oxidation of H₂. A turnover frequency of 1.2 s⁻¹ was observed at 22 °C and 1.0 atm H₂ for catalysis by Cp*Ru(P^{tBu}₂N^{Bn}₂)H. The P^{tBu}₂N^{Bn}₂ ligands are cyclic diphosphine ligands that contain a pendant amine that facilitate intramolecular and intermolecular proton transfers. Addition of water further enhances the turnover frequency to 1.9 s⁻¹. Control experiments on a closely related Ru complex that has no pendant amine show no catalytic activity, and the observed H₂O accelerating effect confirms the critical roles of intramolecular proton relays (the pendant amines) and intermolecular proton relays (H₂O) on the catalytic activity.

Introduction

The interconversion of H⁺, electrons and H₂, i.e. $2\text{H}^+ + 2\text{e}^- \rightleftharpoons \text{H}_2$, is a potentially viable approach to utilize sustainable but intermittent renewable energy resources, such as solar or wind.^{1,2} Interestingly, in the world of bacteria, H₂ also plays an important role in energy storage and metabolism.^{3,4} The metabolism of dihydrogen in bacteria is regulated by a class of metalloenzymes, hydrogenases, including [Ni-Fe] hydrogenase,⁵ [FeFe] hydrogenase⁶ and [mono-Fe] hydrogenase.⁷ The [Ni-Fe] and [FeFe] hydrogenases, which essentially function like the Pt electrode in low temperature fuel cells and electrolyzers for H₂ oxidation and production, have remarkable rates and efficiencies for reversible H₂ oxidation and production. These natural systems have inspired chemists to develop molecular electrocatalysts based on inexpensive

metals for energy conversions.⁸⁻²¹ The [FeFe] hydrogenase enzymes have been shown to contain an azadithiolate ligand at its active site (see Scheme 1) that facilitates H-H formation and heterolytic cleavage,²² and transfers protons between the active site and solution through a proton channel.^{23, 24} Rauchfuss *et al.* incorporated a redox-active derivative of ferrocene into a diiron model complex containing a pendant amine that mimics the [FeFe] hydrogenase active site for the chemical oxidation of H₂.²⁵

Our group has studied a variety of metal complexes containing cyclic diphosphine ligands, abbreviated as P^R₂N^{R'}₂ (1,5-diaza-3,7-diphosphacyclooctane, where R and R' are alkyl or aromatic substituents). The P^R₂N^{R'}₂ ligands have been found to be versatile ligands²⁶⁻²⁹ for the design of nickel,³⁰⁻³³ cobalt^{34, 35} and palladium^{36, 37} electrocatalysts for H₂ production, and nickel^{32, 38-44} and iron⁴⁵⁻⁴⁸ electrocatalysts (see Scheme 1) for hydrogen oxidation. When the pendant amines in the second coordination sphere are positioned close to the metal ion, they play important roles in facilitating the cleavage or formation of the H-H bond and promoting proton transfer between the metal center and solution.

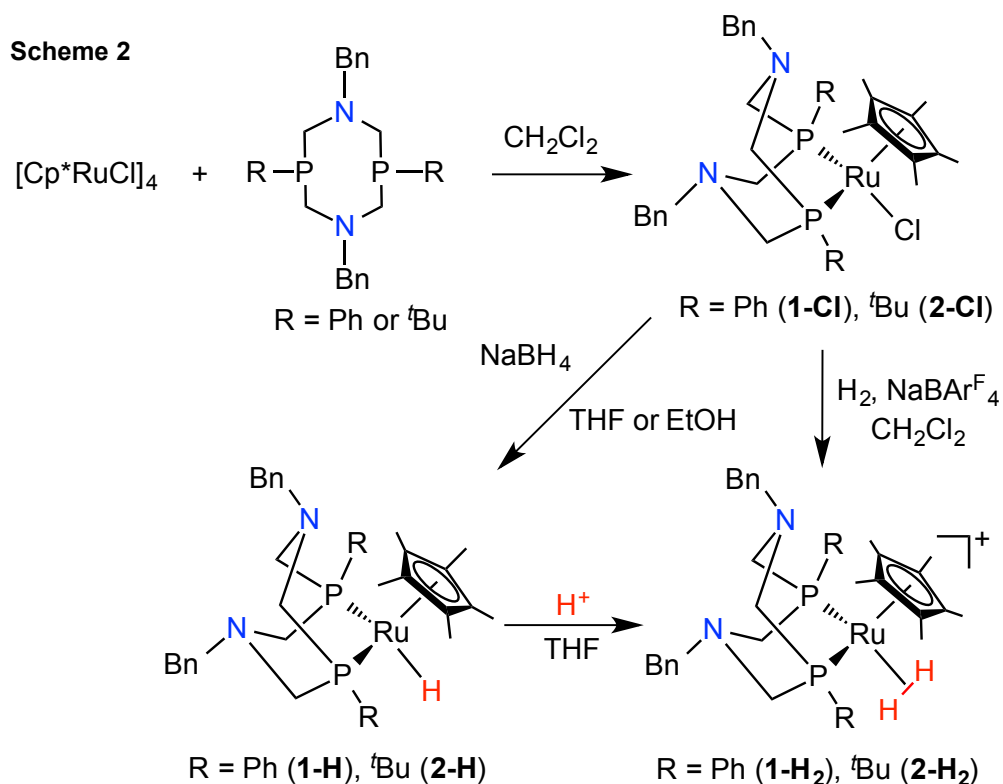


Ruthenium(II) derivatives containing a cyclopentadienyl ligand ($\text{Cp} = \eta^5\text{-C}_5\text{H}_5$) and a diphosphine ligand have been extensively studied, and the facile reactions of these types of complexes with hydrogen under mild conditions to form dihydride and/or dihydrogen derivatives have been well documented.⁴⁹⁻⁵⁴ It has been shown that the activation of H_2 and intramolecular proton transfer in this class of ruthenium complexes is facilitated by a nitrogen base incorporated into monophosphine ligands.⁵⁵ However, electrocatalytic activity for H_2 oxidation or production for these derivatives has not been reported. We have recently reported a half-sandwich Fe complex, $[\text{Cp}^{\text{C}_6\text{F}_5}\text{Fe}(\text{P}^{\text{tBu}}_2\text{N}^{\text{Bn}}_2)\text{H}]$, as the first Fe-based electrocatalyst for H_2 oxidation,⁴⁶ and this result suggests Ru congeners may also be active for electrochemical H_2 oxidation. Mayer and coworkers have shown that $[\text{Cp}^*\text{Ru}(\text{P}^{\text{R}}_2\text{N}^{\text{R}'_2})(\eta^2\text{-O}_2)]\text{PF}_6$ undergoes protonation of one of the pendant amines of the P_2N_2 ligand, forming an intramolecular $\text{O}\cdots\text{H-N}$ hydrogen bond between the pendant amine and the dioxygen ligand, suggesting the pendant amines in the P_2N_2 ligands could also play an important role in catalytic O_2 reduction as observed for $[\text{Ni}(\text{P}^{\text{R}}_2\text{N}^{\text{R}'_2})_2]^{2+}$ complexes.^{56, 57} Although numerous catalysts are known for electrochemical reduction of protons to H_2 ,^{8-21, 26-28, 58} very few molecular electrocatalysts have been developed for H_2 oxidation.^{30, 38, 39, 42, 45-48, 59} We report here the syntheses of new ruthenium complexes, $\text{Cp}^*\text{Ru}(\text{P}^{\text{R}}_2\text{N}^{\text{Bn}}_2)\text{H}$ and $[\text{Cp}^*\text{Ru}(\text{P}^{\text{R}}_2\text{N}^{\text{Bn}}_2)(\text{H}_2)]\text{BAr}^{\text{F}}_4$ [$\text{Bn} = \text{benzyl}$; $\text{Ar}^{\text{F}} = 3,5\text{-bis(trifluoromethyl)phenyl}$] derived from $\text{Cp}^*\text{Ru}(\text{P}^{\text{R}}_2\text{N}^{\text{Bn}}_2)\text{Cl}$ (**1-Cl**, $\text{R} = \text{Ph}$, **2-Cl**, $\text{R} = \text{tBu}$). These studies have led to the development of ruthenium-based electrocatalysts for hydrogen oxidation involving intramolecular heterolytic H-H bond cleavage and further generalize the important functions of pendant amines of the P_2N_2 ligand for intra- and intermolecular proton transfers and H_2 oxidation catalysis.

Results and Discussion

Syntheses of Complexes. Cp*Ru(P^R₂N^{Bn}₂)Cl (**1-Cl**, R = Ph; **2-Cl**, R = ^tBu) (Scheme 2) were synthesized by the reported procedures.^{56, 57} The ¹H NMR and ³¹P NMR spectra of **1-Cl** and **2-Cl** confirmed their identities. When H₂ is bubbled through a dichloromethane-*d*₂ solution of **1-Cl** or **2-Cl** in the presence of NaBAr^F₄ (see Scheme 1), the orange color rapidly fades to pale yellow, and the resulting product is assigned as the dihydrogen complex [Cp*Ru(P^R₂P^{Bn}₂)(H₂)]BAr^F₄, **1-H₂** (R = Ph) and **2-H₂** (R = ^tBu), on the basis of NMR spectroscopic data. The ¹H NMR spectrum of each product shows a broad singlet near -9.0 ppm assigned to the H₂ ligand. No evidence for a second isomer with two hydride ligands is observed in the spectrum. When D₂ is bubbled through the solution of each product, evidence for H-D exchange is observed within minutes, and the HD resonance splits into a triplet with *J*_{H-D} = 20.0 Hz for **1-HD**, and 22.0 Hz for **2-HD**, indicating 0.99 and 1.05 Å H-H bond distances in these molecules according to the equation of Heinekey^{61, 62}. The longer H-H bond distances indicate more activated H₂ molecules in these [Ru(H₂)]⁺ complexes than those of [CpFe^{Ph}₂N^{Bn}₂(H₂)]BAr^F₄⁴⁵ (0.91 Å) and [Cp^{C6F5}Fe^{tBu}₂N^{Bn}₂(H₂)]BAr^F₄⁴⁶ (0.91 Å) calculated by the same equation.⁶² The H-D coupling further confirms that these ruthenium complexes contain dihydrogen ligands. The H-D exchange indicates reversible heterolytic cleavage of H₂ by these ruthenium complexes, consistent with observations previously reported for [CpFe(P^{Ph}₂P^{Bn}₂)(H₂)]BAr^F₄.⁴⁵ This H-D exchange is facilitated by the pendant amine in the ligand, which can lead to the formation of a ruthenium hydride with a protonated base in the ligand, similar to [Cp^{C5F4N}Fe(P^{tBu}₂N^{tBu}₂H)H]BAr^F₄, which was characterized by neutron diffraction studies.⁴⁷ Rapid intermolecular exchange between NH⁺ and ND⁺ sites in the ligands followed by deuteron transfer back to the metal hydride results in the formation of the Ru(H-D) derivative. The [Cp*Ru(P^R₂P^{Bn}₂)(H₂)]BAr^F₄ species are more stable than the corresponding

$[\text{Cp}^*\text{Ru}(\text{P}^{\text{R}}_2\text{N}^{\text{tBu}}_2\text{H})\text{H}]\text{BARF}_4$ tautomers, and are the only species observed experimentally. A similar situation is observed for $[\text{CpFe}(\text{P}^{\text{Ph}}_2\text{P}^{\text{Bn}}_2)(\text{H}_2)]^+$ and its H-H heterolytic cleavage tautomer.⁴⁵ In previous studies of reactions of H_2 with a series of $\text{Cp}^*\text{Ru}(\text{diphosphine})\text{Cl}$ derivatives in the presence of NaBARF_4 , the formation of the dihydride derivative or a mixture of dihydrogen and dihydride isomers was observed by NMR spectroscopy at room temperature.⁵¹⁻⁵⁴ The addition of D_2 to the isomeric mixtures also led to the formation of $\text{Ru}(\text{HD})$ derivatives, but this occurred over a period of hours, significantly slower rate than the rates we observed for **1-H₂** and **2-H₂**.



The reaction of $\text{Cp}^*\text{Ru}(\text{P}^{\text{Ph}}_2\text{N}^{\text{Bn}}_2)\text{Cl}$, **1-Cl**, with excess NaBH_4 in THF gave $\text{Cp}^*\text{Ru}(\text{P}^{\text{Ph}}_2\text{N}^{\text{Bn}}_2)\text{H}$, **1-H**, and a similar reaction of **2-Cl** with NaBH_4 in EtOH resulted in the formation of $\text{Cp}^*\text{Ru}(\text{P}^{\text{tBu}}_2\text{N}^{\text{Bn}}_2)\text{H}$, **2-H** (Scheme 2). The ^1H NMR spectra of these products exhibit triplets (due to the coupling of the hydride ligand to both P atoms of the P_2N_2 ligand,

$J_{\text{PH}} = 30$ Hz) at -12.3 ppm and -14.9 ppm for **1-H** and **2-H**, respectively, that are assigned to the hydride ligands. The addition of $\text{HBF}_4 \cdot \text{Et}_2\text{O}$ to a solution of these metal hydrides in acetone- d_6 resulted in the formation of the corresponding dihydrogen derivatives, **1-H₂** and **2-H₂**, as identified by NMR spectroscopy.

Electrochemical Studies. Cyclic voltammograms for the ruthenium complexes were recorded in 0.1 M $\text{NBu}_4\text{B}(\text{C}_6\text{F}_5)_4$ fluorobenzene solutions, unless otherwise noted, using a glassy carbon electrode. Acetonitrile is often used for electrochemical studies, but these Ru complexes, as well as the related Fe complexes reported earlier, bind CH_3CN strongly, so the non-coordinating solvent fluorobenzene was used in these studies. One-electron oxidations of **1-Cl** and **2-Cl** were observed in CH_2Cl_2 solutions containing 0.1 M Bu_4NPF_6 , and are assigned to the $\text{Ru}^{\text{III/II}}$ couples.⁵⁷ Both complexes exhibit the same potential for the $\text{Ru}^{\text{III/II}}$ couple at -0.38 V versus the ferrocenium/ferrocene couple (all potentials in this paper are reported versus $\text{Cp}_2\text{Fe}^{+/0}$),⁵⁷ implying no substituent effect on the $\text{Ru}^{\text{III/II}}$ redox couple in CH_2Cl_2 solutions. The cyclic voltammogram of the chloride derivative **1-Cl** recorded in fluorobenzene, exhibits a reversible wave of the $\text{Ru}^{\text{III/II}}$ couple at -0.44 V ($\Delta E_p = 85$ mV) (see Figure 2a), ca. 60 mV more negative than the value recorded in CH_2Cl_2 . No reduction wave was observed at potentials as negative as -2.0 V. **2-Cl** exhibits a reversible $\text{Ru}^{\text{III/II}}$ couple at -0.48 V, 40 mV more negative than that of **1-Cl**, suggesting the $\text{P}^{\text{tBu}}_2\text{N}^{\text{Bn}}_2$ ligand is slightly more electron donating than $\text{P}^{\text{Ph}}_2\text{N}^{\text{Bn}}_2$ (See Figure 2c), consistent with Ni(I/0) couples for complexes with these ligands.⁶⁴ Plots of the anodic peak current versus the square root of the scan rate are linear, indicating the oxidations of **1-Cl** and **2-Cl** are diffusion-controlled one-electron processes (See Figures S1 and S2).

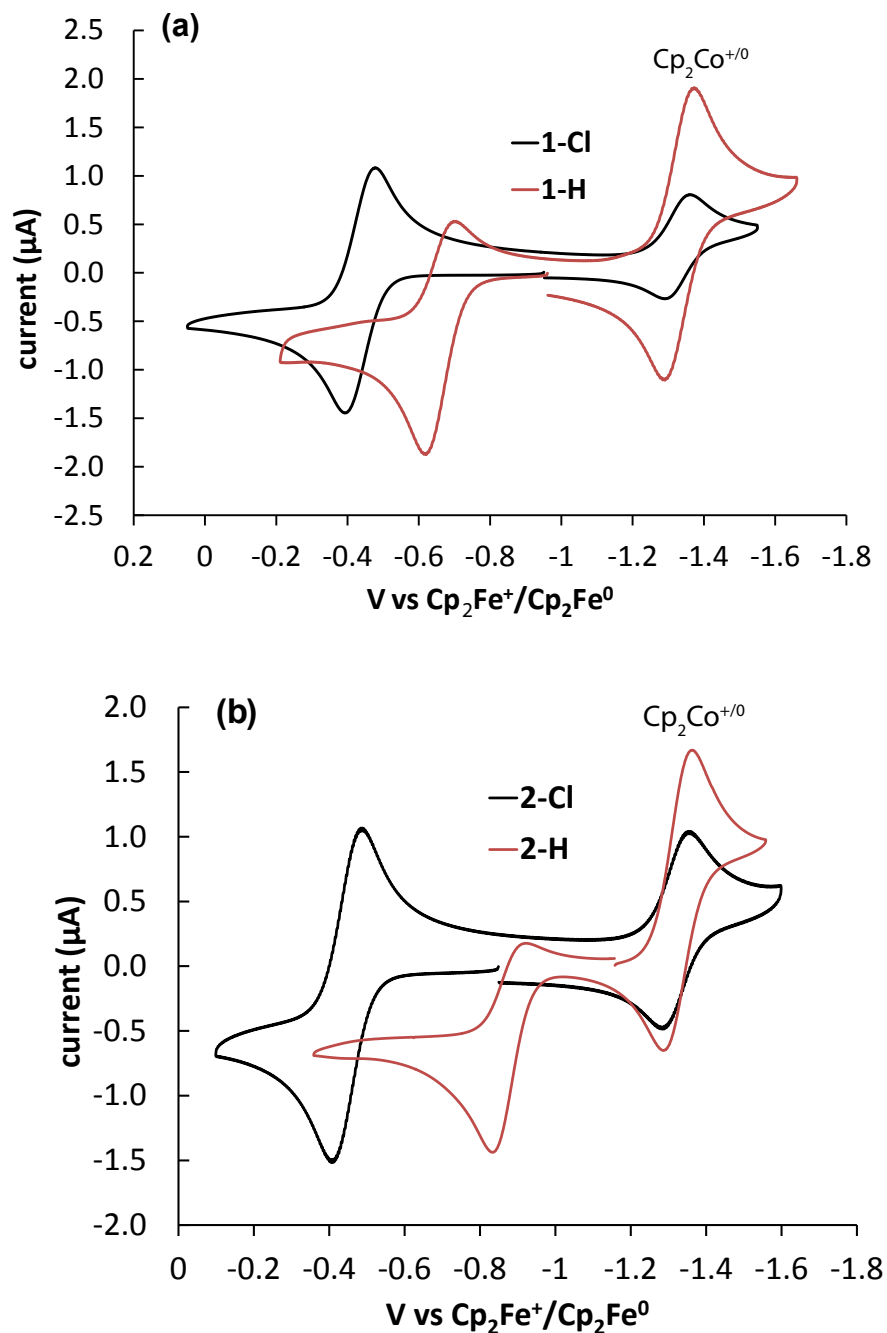


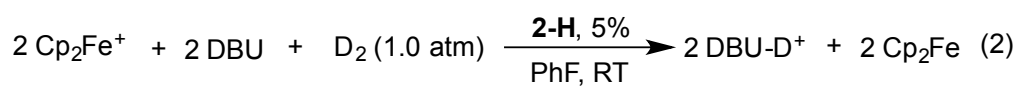
Figure 1. (a) Cyclic voltammograms of **1-Cl** (black trace) and **1-H** (red trace); (b) Cyclic voltammograms of **2-Cl** (black trace) and **2-H** (red trace). Conditions: 1.0 mM [Ru]; 0.1 M ⁿBu₄NB(C₆F₅)₄; under 1.0 atm Ar; scan rate, 100 mV/s; Cp₂CoPF₆ (-1.33 V vs Cp₂Fe⁺⁰) was used as an internal reference and is present in all four cyclic voltammograms.

In the cyclic voltammogram of the hydride derivative **1-H**, the quasi-reversible wave corresponding to the Ru^{III/II} couple (anodic peak at -0.62 V) is shifted to a more negative value relative to that of the chloride derivative (-0.44 V). Scan rate dependence studies in a range from 0.1 V/s to 25.0 V/s revealed that the oxidation becomes fully reversible above 16.0 V/s (see Figure S3). In the cyclic voltammogram of **2-H**, which contains the more electron-donating ^tBu group on the phosphorus atoms, the Ru^{III/II} oxidation was shifted to a significantly more negative potential of -0.84 V in fluorobenzene. This oxidation wave showed quasi-reversible character that was scan-rate dependent; at a scan rate of 100 mV/sec a small reduction peak was observed upon reversing the initial scan direction with $i_a/i_c = 1.8$, and at a scan rate of 25 V/sec, the i_a/i_c ratio was ca. 1.0 (see Figure S4). The irreversible character of the oxidation of **1-H** and **2-H** at slow scan rates is attributed to irreversible chemical reactions following the oxidation of Ru^{II}H to Ru^{III}H: facile intramolecular proton transfer from the Ru center to a pendant base and subsequent intermolecular proton transfer to Ru^{II}H, which is consistent with electrochemical behavior of half-sandwich Fe-hydrides with similar ligand environments, e.g. Cp^{C6F5}Fe(P^{tBu}₂P^{Bn}₂)H.^{45, 46}

Both complexes **1-H** and **2-H** were examined for electrochemical H₂ oxidation (1.0 atm). Under an atmosphere of H₂, no change was observed in the potential or the amplitude of the oxidation wave at -0.62 V, the Ru^{III/II} couple of **1-H**. This indicates that neither the starting metal hydride **1-H** nor its oxidized form reacts rapidly with H₂. However, when aliquots of the amine base DBU (1,8-diazabicyclo[5.4.0]undec-7-ene, p*K*_a = 24.34 for H-DBU⁺ in CH₃CN)⁶⁵ were added to this solution under hydrogen, an increase in oxidizing current was observed at a slightly more negative potential (half peak potential at -0.71 V) with the wave reaching a plateau after the addition of about 8.0 equiv of base. This current increase is characteristic of an electrocatalytic oxidation of H₂. The cathodic shift of the catalytic waves of **1-H** compared to the

original oxidation wave suggests that proton transfer following oxidation is fast in the presence of DBU. At concentrations of base greater than 6.0 mM, the catalytic current becomes independent of base concentration, and the ratio of the catalytic current (i_{cat}) to the peak current in the absence of H₂, (i_p) is 3.6 (see Figure S5) at a scan rate of 20 mV/s. This ratio can be used to calculate a turnover frequency for H₂ oxidation of 0.6 s⁻¹ under 1.0 atm of H₂ at room temperature using equation 1, where n is the number of electrons (2 for H₂ oxidation), R is the gas constant (8.314 J K⁻¹ mol⁻¹), F is Faraday's constant (9.65×10^4 C/mol), and T is the temperature (298 K).⁶⁶⁻⁶⁸ Electrochemical H₂ oxidation using complex **2-H** as electrocatalyst gave a rate of 1.2 s⁻¹, ca. twice that of **1-H**. The catalytic oxidation of H₂ has been confirmed by identifying the deuterated base, DBU-D⁺ (at 10.54 ppm in the ²H NMR spectrum) in the chemical oxidation of D₂ employing **2-H** as the catalyst and ferrocenium as the oxidant (see equation 2). The yield of deuterons from the chemical oxidation of D₂ catalyzed by **2-H** corresponded to 9.2 turnovers, confirming catalysis. The turnover frequencies for the oxidation of H₂ catalyzed by **1-H** and **2-H** are comparable to that of recently reported Cp^{C6F5}Fe(P^{tBu}₂P^{Bn}₂)H.⁴⁶ From the pK_a of the conjugate acid of the exogenous base, DBU, the catalytic overpotential at $E_{cat/2}$ for **1-H** and **2-H** can be estimated to be 0.6 and 0.5 V, respectively. The estimation of the overpotential is based on the pK_a difference of DBU and Et₃N in CH₃CN (see details in the Supporting Information). Other bases such as methypyrrolidine and triethylamine did not lead to catalysis of H₂ oxidation.

$$k_{obs} = \text{TOF} = \frac{0.1992Fv}{n^2RT} \left(\frac{i_{cat}}{i_p}\right)^2 \quad (1)$$



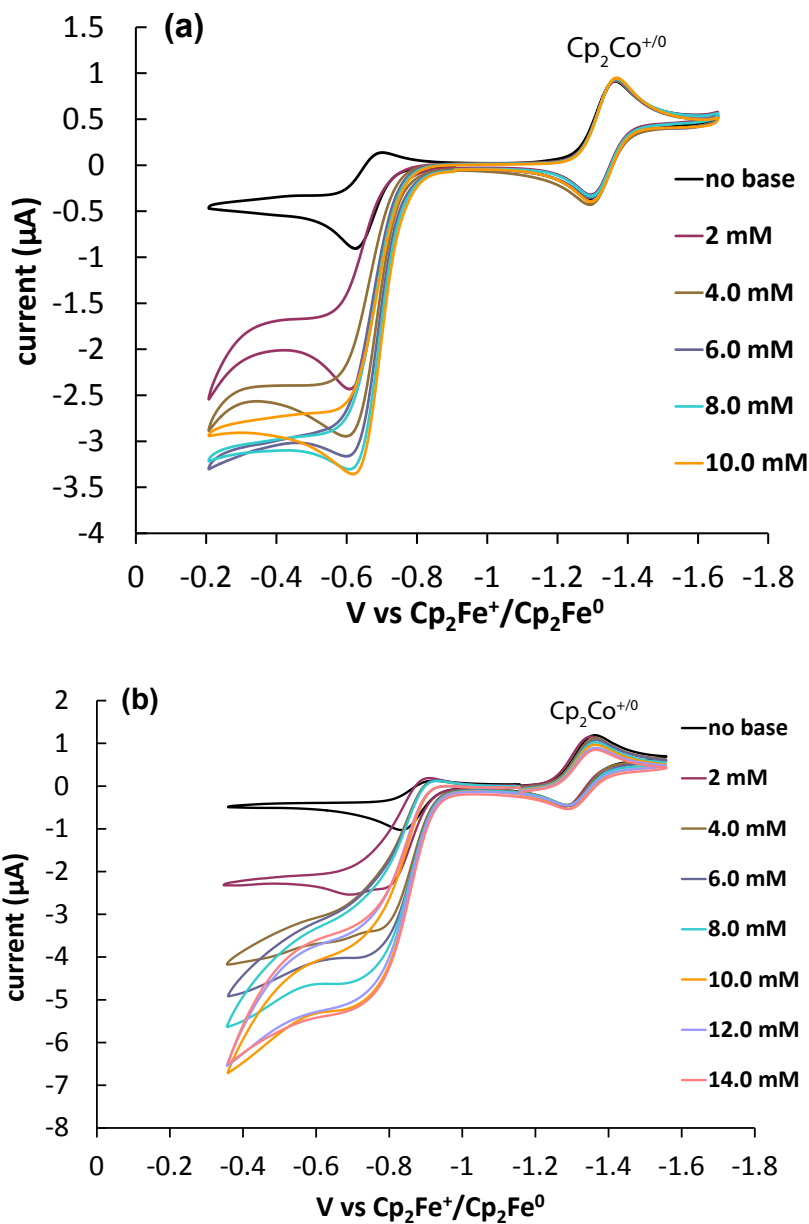
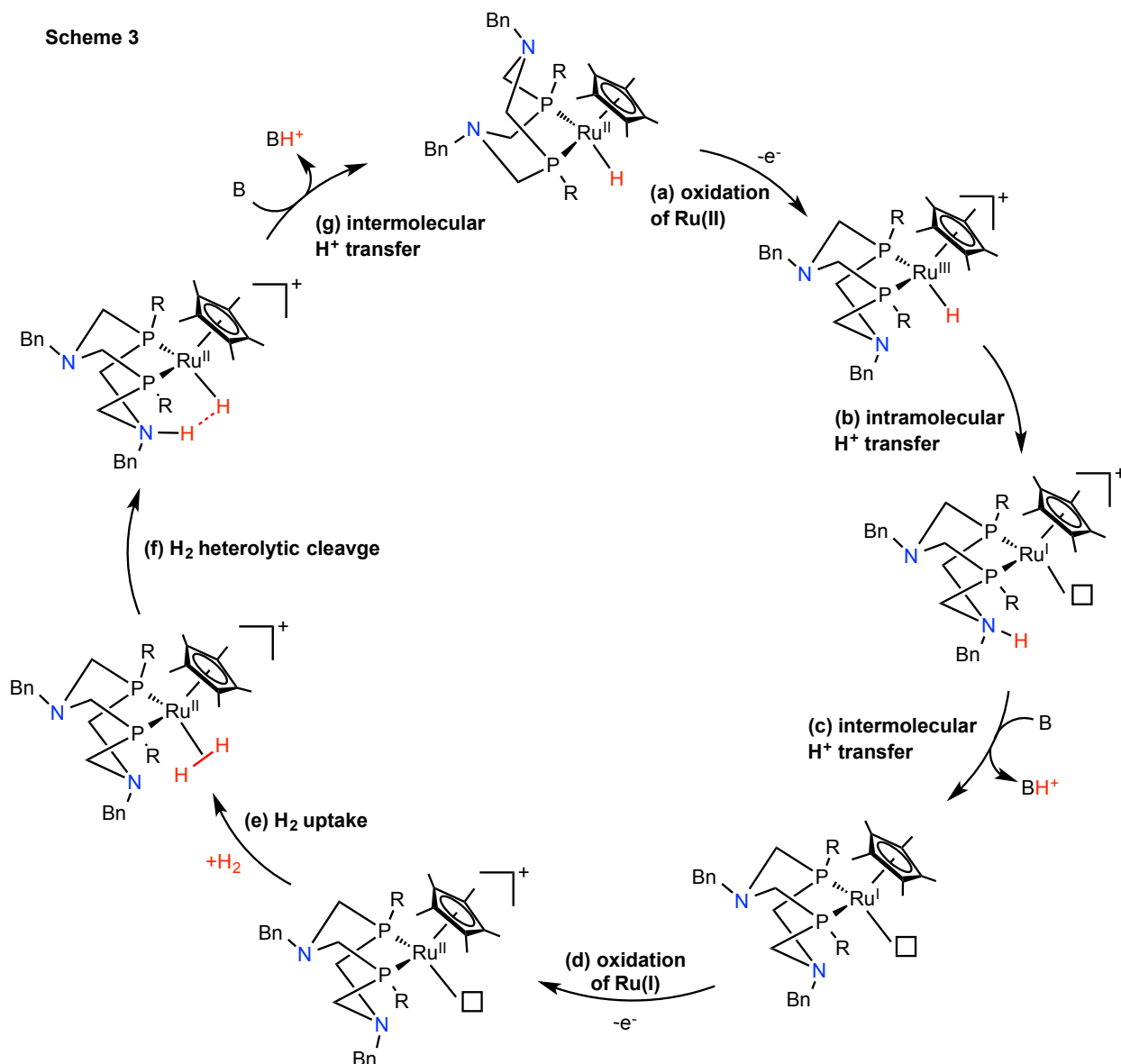


Figure 3. Electrochemical H₂ oxidation by **1-H** and **2-H**. (a) Cyclic voltammograms of a fluorobenzene solution of **1-H** (1.0 mM) under 1.0 atm H₂ with increasing concentrations of DBU as indicated in the legend. (b) Cyclic voltammograms of a fluorobenzene solution of **2-H** (1.0 mM) under 1.0 atm H₂ with increasing concentrations of DBU as indicated in the legend. Conditions: 1.0 mM Ru hydride ; 0.1 M ⁿBu₄NB(C₆F₅)₄; 1.0 atm H₂; scan rate, 20 mV/s; 22 °C; Cp₂CoPF₆ (-1.33 V) as internal reference.

Based on the data presented above, a catalytic cycle for oxidation of H₂ is proposed in Scheme 3 for the catalytic oxidation of H₂ by **1-H** and **2-H**. This mechanism is the analogous to that proposed for related half-sandwich complexes of Fe that also contain P₂N₂ ligands.⁴⁶ In this mechanism, H₂ oxidation is initiated by oxidation of the Ru^{II} hydride (step a) followed by facile intramolecular proton transfer from the Ru^{III}-H to the pendant amine (step b); the square in Scheme 3 indicates a vacant coordination site on the metal. Deprotonation by the exogenous base, DBU (step c) gives a Ru^I species that undergoes a second oxidation to produce an unsaturated Ru^{II} species (step d) that binds H₂ (step e). We propose an intramolecular heterolytic H₂ cleavage (step f) that leads to a Ru hydride and protonated amine. This complex is shown in Scheme 3 with a “dihydrogen bonding” interaction^{69, 70} between the protic N-H^{δ+} and hydridic Ru-H^{δ-}. We recently isolated a related Fe-H•••H-N complex, and its structure was determined by single crystal neutron diffraction.⁴⁷ Intermolecular deprotonation of the Ru-H•••H-N intermediate provides a lower barrier pathway compared to direct deprotonation of the Ru-(H₂) complex. The existence of the Ru(H₂) complex and its H₂ cleavage tautomer (the intermediate formed in step f) is supported by H₂/D₂ scrambling observed for **1-H₂** and **2-H₂**.^{45, 46} Collman *et al.* previously reported a mononuclear Ru^{II} porphyrin complex, Ru(OEP)(THF)₂ (OEP = octaethylporphinato dianion) that is an electrocatalyst for H₂ oxidation when absorbed on the edge planes of graphite electrodes.⁷¹ Ogo *et al.* previously reported a Ni-Ru heterobimetallic complex as a H₂ oxidation catalyst and demonstrated its function in a PEM fuel cell device.⁷² For both Ru based catalysts, which lack a built-in base, catalysis is proposed to involve intermolecular heterolysis of H₂ using an exogenous base during the oxidation of H₂.



Effect of H₂O on H₂ oxidation by 1-H and 2-H

For Ni-based H₂ oxidation electrocatalysts, H₂O can significantly accelerate the rate of intermolecular proton transfer from the protonated pendant base to a base in solution.^{41, 42} This can lead to different catalytic pathways under different conditions. In the presence of water, deprotonation of the protonated pendant amine prior to oxidation leads to a lower overpotential compared to a pathway where oxidation precedes proton transfer.⁴² To determine if water might influence the turnover frequencies or overpotentials for oxidation of H₂ by **1-H** and **2-H**, water

was added to form a saturated fluorobenzene solution at a base (DBU) concentration of 14.0 mM (i.e. in the base independent concentration regime). In the case of **1-H**, addition of H₂O led to a decrease in the catalytic current (See Figure S6). However, for **2-H**, a modest catalytic current enhancement was observed upon addition of 20 μ L water with $i_{\text{cat}}/i_{\text{p}} = 6.6$, corresponding to a turnover frequency of 1.9 s⁻¹ (see Figure 4). This rate is ca. 1.6 times faster than without added H₂O for this Ru complex.^{41,42} In addition to the enhanced current, there is an apparent cathodic shift in the half-wave potential (ca. 40 mV). This shift indicates that proton transfer from the Ru^{III}H to the base in solution is faster for this complex in the presence of water. This observation is consistent with a steric component to the activation barrier associated with the intermolecular proton transfer shown in step c of Scheme 3 that is decreased by water bridging between the protonated pendant base and the base in solution. Further addition of H₂O to the solution of **2-H** did not lead to any additional increase in the catalytic current or decrease in overpotential, consistent with saturation of the fluorobenzene solution.

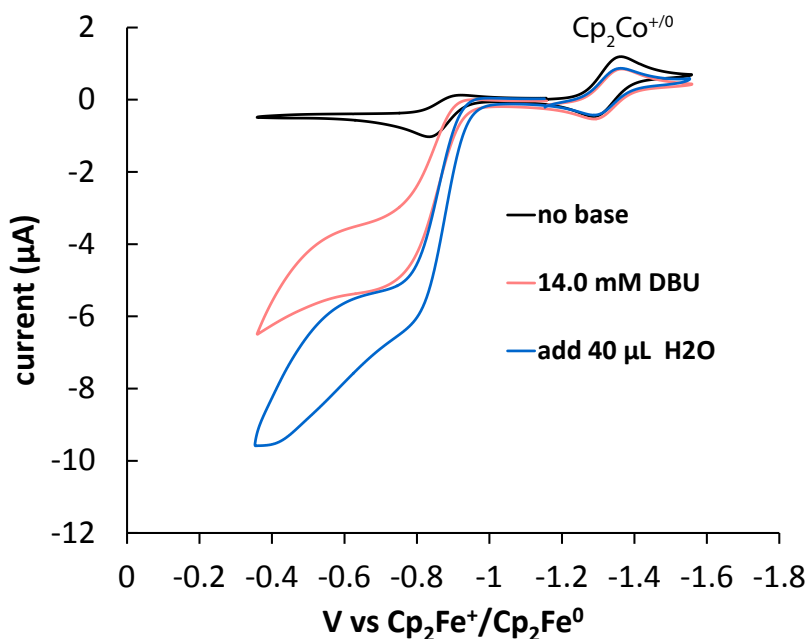
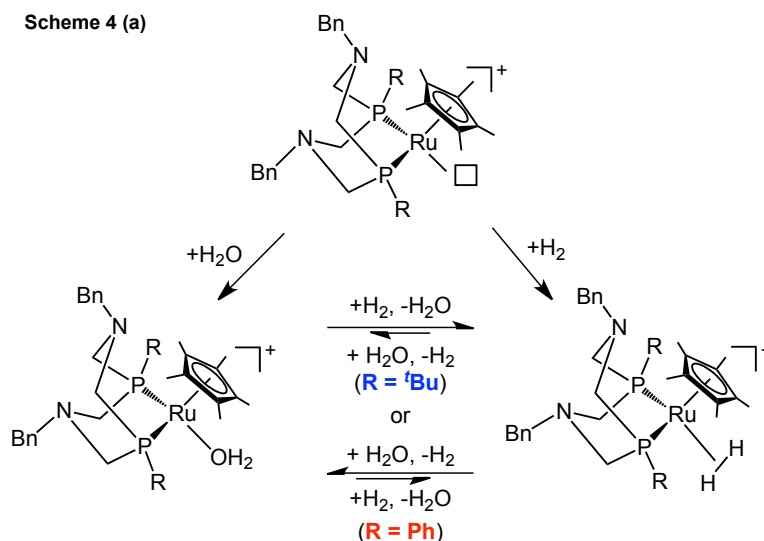


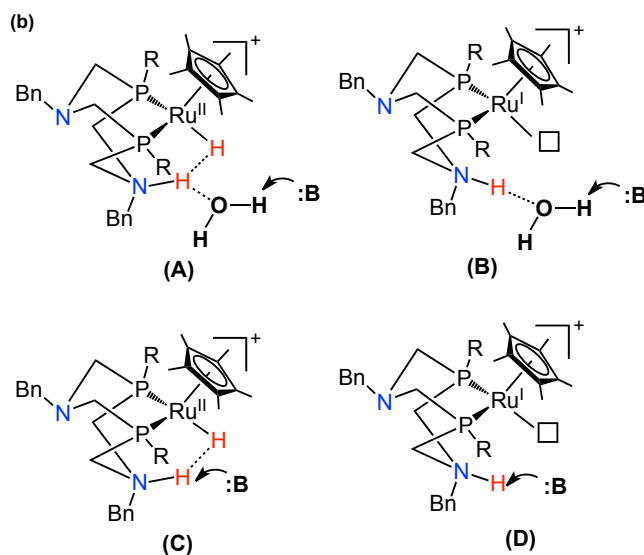
Figure 4. Electrochemical H₂ oxidation by **2-H** before and after addition of 20 μL H₂O into 1.0 mL of fluorobenzene solution. Conditions: fluorobenzene solution, 1.0 mM **2-H**; 0.1 M ⁿBu₄NB(C₆F₅)₄; 1.0 atm H₂; scan rate, 20 mV/s; 22 °C; Cp₂CoPF₆ (-1.33 V) as internal reference.

One plausible explanation for the different observations of the effect of H₂O for **1-H** and **2-H** is that the preference for binding H₂ and H₂O is different for the unsaturated Cp*Ru(P₂N₂)⁺ complexes formed in step d in Scheme 3. Several Ru(H₂O) half-sandwich complexes supported with Cp or Cp* ligands have been structurally characterized by single crystal X-ray diffraction.^{73, 74} Competitive binding of H₂ vs H₂O has also been studied for several dihydrogen complexes. In early studies, Kubas and co-workers found that the relative binding strength of H₂ vs H₂O to tungsten complexes varies according to temperature.⁷⁵ A recent review discusses the influence of hydrogen bonding, solvent, and entropic factors that influence the relative strength of binding of H₂ vs H₂O.⁷⁶ For **1-H** we hypothesize that the open site of the unsaturated species preferentially coordinates H₂O over H₂. Because of this competitive binding of H₂O, only a small amount of **1-H**₂ enters into the catalytic cycle, leading to the observation of decreased catalytic current. In the case of **2-H**, it is believed the relative binding ability of H₂O and H₂ is reversed due to subtle differences in the Lewis acidity of the unsaturated species or the polarity of the binding pocket, arising from the different phosphorus substituents, phenyl versus *t*-butyl. In this case, the rate of H₂ binding (step e of Scheme 3) and the rate of intermolecular proton transfer (step c) are faster, leading to a small increase in rate and a small decrease in the overpotential.

Complex **A** of Scheme 4b corresponds to the heterolytic cleavage product of H₂ (step g in Scheme 3) and complex **B** of Scheme 4b corresponds to the Ru^I species resulting from intramolecular proton transfer in step b of Scheme 3. In Scheme 4b, H₂O can assist proton transfer by forming hydrogen bonds with the two catalytic intermediates, **A** and **B**, and the

exogenous base (denoted as :B) can remove a proton from the bridging water molecule that may function as a secondary proton relay.⁴² The formation of the intermediate **B** is consistent with the potential shift of the catalytic current (see Figure 4). Compared to the direct proton transfer from the catalyst to an exogenous base (complexes **C** and **D** in scheme 4(b)), proton transfer through a bridging H₂O molecule is believed to have a lower barrier, with reduced steric hindrance and greater accessibility of the exogenous base. In contrast, for Cp^{C6F5}Fe(P^{tBu}₂P^{Bn}₂)H,⁴⁶ which has a similar ligand environment as **1-H** and **2-H**, addition of H₂O completely inhibits the oxidation of H₂. It should be noted water tolerance is a prerequisite for H₂ oxidation catalysts in fuel cell applications as there is a large humidity at both electrode sides of proton exchange membrane (PEM) fuel cell devices. Further understanding of the H₂O compatibility of **2-H** could lead to the development of H₂O tolerant Fe catalysts.





Comparative Studies of Cp*Ru(dmpm)H. The ability of Cp*Ru(P^tBu₂N^{Bn}₂)H to serve as an electrocatalyst for oxidation of H₂ is attributed to the ability of the pendant amine to function as an effective proton relay for intramolecular proton transfers, including heterolytic cleavage of H₂, and for proton transfers to the exogenous base in solution. A related ruthenium complex that does not incorporate a proton relay was also studied for possible electrocatalytic activity. Cp*Ru(dmpm)Cl (where dmpm = bis(dimethylphosphino)methane) is expected to have an electronic influence at the metal center similar to P₂N₂ ligands. Cp*Ru(dmpm)Cl was synthesized according to a published procedure,^{77, 78} and converted to Cp*Ru(dmpm)H by a reaction with excess NaBH₄ in ethanol.

Cp*Ru(dmpm)Cl exhibits a reversible Ru^{III/II} wave at -0.52 V, which is 40 mV more negative than that of **2-Cl** (see Figure S7). Scan rate dependence studies indicate the oxidation is a diffusion-controlled one-electron process (see Figure S8). Cp*Ru(dmpm)H shows an irreversible oxidation peak at -0.61 V at 100 mV/s (see Figure S9). Under H₂ (1.0 atm) and in the presence of DBU, there is a current enhancement by a factor of about 2 consistent with the H⁺ ligand being oxidized to a proton, but there is no plateau in current (see Figure S10) that would

indicate catalytic H₂ oxidation. This control experiment indicates that the pendant amine is required for the catalytic H₂ oxidation observed for **1-H** and **2-H**.

Remarks on the Ru Catalysts and Previously Reported Fe Catalysts. The design of Ru-hydride catalysts, **1-H** and **2-H**, was inspired by previously reported Fe catalysts, [Cp^{C6F5}Fe(P^{tBu}₂N^{Bn}₂)H]⁴⁶ and [Cp^{C5F4N}Fe(P^{tBu}₂N^{tBu}₂H)H]BAr^F₄.⁴⁷ Both Ru and Fe catalysts have a similar piano-stool geometry. There are subtle differences in the ligand environment for these two systems. Complex **1-H**, Cp*Ru(P^{Ph}₂N^{Bn}₂)H, is more similar to CpFe(P^{Ph}₂N^{Bn}₂)H⁴⁵ as they share the same P₂N₂ ligand. The Fe complex is not catalytic for the oxidation of H₂ due to base (DBU) binding to the open site of the corresponding unsaturated species, [CpFe(P^{Ph}₂N^{Bn}₂)]⁺.⁴⁵ It is believed that the observed catalysis by **1-H** benefits from the steric protection provided by the bulky Cp* ligand that impedes DBU binding. **2-H**, Cp*Ru(P^{Ph}₂N^{Bn}₂)H, is more closely related to [Cp^{C6F5}Fe(P^{tBu}₂N^{Bn}₂)H]⁴⁶ with the major difference being the substituents on the Cp ring. In terms of electrochemical oxidation of H₂, **1-H** and **2-H** exhibited similar rates to the Fe catalysts but higher overpotentials. The larger overpotentials for **1-H** and **2-H** are due to the use of the stronger exogenous base (DBU) compared to weaker bases (e.g. N-methylpyrrolidine and Et₃N) used for the Fe catalysts. As mentioned above, complexes **1-H** and **2-H** did not show catalysis using N-methylpyrrolidine and Et₃N. While Ru metal is more electronegative than Fe, Cp* is much more electron-donating than Cp^{C6F5} and Cp^{C5F4N}, and the Cp*Ru(H₂) complexes are more basic than the Fe(H₂) complexes supported by Cp^{C6F5} or Cp^{C5F4N} ligands. As a result, intermolecular deprotonation of **1-H** and **2-H** (step g in Scheme 3) cannot be accomplished using weak bases.

Summary / Conclusions

A new class of Ru electrocatalysts containing P_2N_2 ligands with pendant amines have been developed for electrochemical H_2 oxidation, demonstrating the general utility of pendant bases in the design of molecular electrocatalysts for H_2 oxidation and production for a range of metals. Our studies of a control complex lacking the pendant amines indicates the pendant amines are crucial to function as proton relays in the catalytic oxidation of H_2 . In addition, structural changes of the ligand can influence catalytic activity by influencing the binding affinity of H_2 and H_2O , and suggest similar control may be feasible for related Fe-H catalysts through systematic ligand modification.

Experimental Section

General Experimental Procedures. 1H , 2H and $^{31}P\{^1H\}$ NMR spectra were recorded on a Varian Inova spectrometer (500 MHz for 1H) at 20 °C. All 1H chemical shifts have been internally calibrated to the monoprotio impurity of the deuterated solvent. The $^{31}P\{^1H\}$ NMR spectra were proton decoupled and are referenced to external phosphoric acid.

All electrochemical experiments were carried out under an atmosphere of argon or hydrogen as indicated, in 0.1 M $nBu_4NB(C_6F_5)_4$ fluorobenzene electrolyte solutions. Cyclic voltammetry experiments were performed with a CH Instruments model 660C potentiostat. Cobaltocenium hexafluorophosphate (Cp_2CoPF_6) was used as a secondary internal standard with all potentials referenced to the Cp_2Fe^+/Cp_2Fe^0 couple at 0 V. The working electrode (1 mm PEEK-encased glassy carbon, Cypress Systems EE040) was polished using Al_2O_3 (BAS CF-1050, dried at 150 °C under vacuum) suspended in fluorobenzene, and then rinsed with neat fluorobenzene. A glassy carbon rod (Structure Probe, Inc.) was used as the counter electrode. The reference electrode consisted of a silver wire coated with a layer of AgCl and suspended in a solution of

0.1 M ${}^t\text{Bu}_4\text{NB}(\text{C}_6\text{F}_5)_4$ in fluorobenzene. The solution of the reference electrode was separated from the analyte solution by a Vycor frit.

Synthesis and Materials. All reactions and manipulations were performed under an Ar or H_2 atmosphere using standard Schlenk techniques or a glovebox. Solvents were dried using an activated alumina column and stored under Ar. *N*-methylpyrrolidine, Et_3N , and DBU (1,8-diazabicyclo[5.4.0]undec-7-ene) were distilled from KOH and stored under Ar. All NMR solvents were purified according to standard methods. 1,3-di(*t*-butyl)-5,7-dibenzyl-1,5-diaza-3,7-diphosphacyclooctane ($\text{P}^{\text{tBu}}_2\text{N}^{\text{Bn}}_2$),⁶⁴ 1,3-diphenyl-5,7-dibenzyl-1,5-diaza-3,7-diphosphacyclooctane ($\text{P}^{\text{Ph}}_2\text{N}^{\text{Bn}}_2$)³⁰, $\text{Cp}^*\text{Ru}(\text{P}^{\text{Ph}}_2\text{N}^{\text{Bn}}_2)\text{Cl}$ (**1-Cl**),⁵⁷ $\text{Cp}^*\text{Ru}(\text{P}^{\text{tBu}}_2\text{N}^{\text{Bn}}_2)\text{Cl}$ (**2-Cl**)⁵⁷ and $\text{Cp}^*\text{Ru}(\text{dmpm})\text{Cl}$ ^{77, 78} were prepared using published procedures. All other reagents were used as received.

$[\text{Cp}^*\text{Ru}(\text{P}^{\text{Ph}}_2\text{N}^{\text{Bn}}_2)(\text{H}_2)]\text{BAr}^{\text{F}_4}$ (1-H₂**).** $\text{Cp}^*\text{Ru}(\text{P}^{\text{Ph}}_2\text{N}^{\text{Bn}}_2)\text{Cl}$ (0.022 g, 0.03 mmol) was dissolved in a CD_2Cl_2 solution that had been purged with H_2 . A solution of $\text{NaBAr}^{\text{F}_4}$ (0.027 g, 0.03 mmol) in CD_2Cl_2 was purged with H_2 and added to the ruthenium complex. The color of the solution mixture changed to pale yellow. The dihydrogen adduct was identified by NMR spectroscopy. Attempts to evaporate solvent to isolate the complex lead to decomposition, presumably due to loss of H_2 . ${}^1\text{H}$ NMR, (CD_2Cl_2 , ppm): -8.59 (br s, 2 H, Ru- H_2); 1.42 (s, 15H, Cp*); 3.29, 3.24, 2.94, 2.60 (m, 8H, CH_2); 3.98, 3.66 (s, 2 H each, CH_2Ph); 7.0-7.8 (m, Ar-H, 20 H). ${}^{31}\text{P}\{^1\text{H}\}$ NMR (CD_2Cl_2 , ppm): 34.62 (s).

$[\text{Cp}^*\text{Ru}(\text{P}^{\text{tBu}}_2\text{N}^{\text{Bn}}_2)(\text{H}_2)]\text{BAr}^{\text{F}_4}$ (2-H₂**).** Complex **2-H₂** was generated analogous to **1-H₂**. ${}^1\text{H}$ NMR, (CD_2Cl_2 , ppm): -9.89 (br s, 2 H, Ru- H_2); 1.04 (3-line pattern, 18 H, t-Bu); 1.92 (s, 15 H, Cp*); 2.45 (m, 6 H, CH_2); 2.80 (br, m, 2 H, CH_2); 3.67, 3.64 (s, 2 H each, CH_2Ph); 7.2-7.8 (m, Ar-H, 22 H). ${}^{31}\text{P}\{^1\text{H}\}$ NMR (CD_2Cl_2 , ppm): 45.32 (s).

1-H₂ and **2-H₂** can also be prepared by addition of one equivalent of HBF₄·Et₂O to the corresponding Ru-H species in acetone.

[Cp*Ru(P^{tBu}₂N^{Bn}₂)(HD)]BAR^F₄ (2-HD) [Cp*Ru(P^{tBu}₂N^{Bn}₂)(H₂)]BAR^F₄ in CD₂Cl₂ was purged with D₂ for ca. 5 minutes. In the ¹H NMR spectrum, both the original Ru(H₂) resonance and a new triplet near -9.9 ppm with $J_{\text{HD}} = 22.0$ Hz were observed and is assigned to the Ru(HD) resonance.

Cp*Ru(P^{Ph}₂N^{Bn}₂)H (1-H). Under a N₂ atmosphere, Cp*Ru(P^{tBu}₂N^{Bn}₂)Cl (0.212 g, 0.3 mmol) was dissolved in ca. 10 mL THF and the resulting solution was added to a suspension of NaBH₄ (0.114 g, 3.0 mmol, in 10 mL ethanol). The color immediately changed from orange to yellow. The solution was stirred for 3 h, then the pale yellow precipitate was collected by filtration and dried. Recrystallization of the product from Et₂O yields an analytically pure product. ¹H NMR, (C₆D₆, ppm): -12.3 (t, $J_{\text{PH}} = 30$ Hz, 1 H, Ru-H); 1.77 (s, 15 H, Cp*); 3.18, 2.95, 2.90, 2.50 (m, 2 H each, CH₂); 3.87, 3.21 (s, 2 H each, CH₂Ph); 7.0-7.5 (m, Ph, 20 H). ³¹P{H} NMR (C₆D₆, ppm); 44.09 (s). Anal. Calcd. for C₄₀H₄₈N₂P₂Ru: Calc. C, 66.74; H, 6.72; N, 3.89. Found: C, 66.32; H, 6.31; N, 3.54.

Cp*Ru(P^{tBu}₂N^{Bn}₂)H, (2-H). Under a N₂ atmosphere, Cp*Ru(P^{tBu}₂N^{Bn}₂)Cl (0.212 g, 0.3 mmol) was dissolved in ca. 20 mL EtOH, and NaBH₄ (0.114 g, 3.0 mmol) was added. The color of the solution immediately changed from orange to yellow. The solution was stirred for 3 h, then the pale yellow precipitate was collected by filtration and dried. This product was redissolved in Et₂O, the solution filtered, and after solvent removal under vacuum, the resulting solid was dried again. Yield: 0.10 g, 50%. ¹H NMR, (C₆D₆, ppm): -14.94 (t, $J = 31$ Hz, 1 H, Ru-H); 1.01 (t, 18 H, t-Bu); 2.09 (s, 15 H, Cp*); 1.89, 2.21, 2.32, 3.1 (m, 2 H each, CH₂); 3.39, 3.75

(s, 2 H each, CH₂Ph); 7.0-7.5 (m, Ph, 10 H). ³¹P{H} NMR (C₆D₆, ppm); 52.44 (s). Anal. Calcd. for C₃₆H₅₆N₂P₂Ru: Calc. C, 63.60; H, 8.30; N, 4.12. Found: C, 63.23; H, 8.48; N, 4.17.

Cp*Ru(dmpm)H. Cp*Ru(dmpm)Cl (0.077 g, 0.19 mmol) was dissolved in EtOH and NaBH₄ (0.086 g, 2.3 mmol) was added. The solution was stirred for 20 h, and then evaporated to dryness. The yellow solid was extracted with Et₂O, the resulting yellow solution was filtered, and after solvent removal from the filtrate the resulting solid was dried under vacuum. The extraction/filtration process was repeated to give the product as a yellow brown solid. Yield: 0.056 g, ca. 80%. ¹H NMR (ppm, d₈-tol): -11.28 (t, 1 H, Ru-H, *J*_{PH} = 34 Hz); 3.01 (m, 1 H, CH₂); 2.63 (m, 1 H, CH₂); 2.11 (t, 15 H, Cp*, *J*_{PH} = 2 Hz); 1.31 (t, *J*_{PH} = 5 Hz, 6H, Me); 1.26 (t, *J*_{PH} = 4 Hz, 6 H, Me). ³¹P{¹H} NMR (d₈-toluene): -14.56 (s). Anal. Calcd. for C₁₅H₃₀RuP₂: Calc. C, 48.25; H, 8.30. Found: C, 48.17; H, 8.03.

Electrochemical H₂ Oxidation Catalyzed by 1-H and 2-H. A 1.0 mL fluorobenzene solution containing 1.0 mM catalyst (**1-H** or **2-H**) was maintained under 1.0 atm hydrogen. Aliquots of base (DBU) were added, and the cyclic voltammograms were recorded after each addition. The peak current observed for the oxidation of **1-H** or **2-H** in the absence of base is defined as *i*_p for **1-H** or **2-H**, and the peak or plateau current observed in the presence of various amounts of base is *i*_{cat}. The ratio of *i*_{cat}/*i*_p was used to determine the rate for the oxidation of H₂. The effect of H₂O on the oxidation of H₂ was examined by adding H₂O to the solution of **1-H** or **2-H** after reaching the base-concentration independent regime.

Chemical Oxidation of D₂ Catalyzed by 2-H. Chemical oxidation of D₂ was conducted to establish the catalytic nature of electrochemical H₂ oxidation. This evaluation using D₂ instead of H₂ avoids interference of any adventitious protons that could possibly occur during H₂ chemical oxidation. A standard solution of C₆D₆ (10 mM) was prepared in PhF. A solution of **2-H** (5.0

mM) was prepared using the standard solution. For each individual experiment, 5% loading of **2-H** (1.0 mL, 3.34 mg, 0.005 mmol) was added to a NMR tube with the preloaded oxidant, $[\text{Cp}_2\text{Fe}]\text{PF}_6$ (27 mg, 0.1 mmol) under D_2 (1.0 atm). Then 0.1 mmol DBU (16 μL) was injected into the NMR tube. The NMR tube was shaken for ca. 5 min, resulting in an orange solution and the disappearance of the blue color associated with $[\text{Cp}_2\text{Fe}]\text{PF}_6$. Subsequently, a ^2H NMR spectrum was recorded to verify the formation of deuterated base, $[\text{DBU-D}]\text{PF}_6$, with a ^2H NMR resonance at 10.54 ppm. The average yield of the product $[\text{DBU-D}]\text{PF}_6$ from two runs was ca. 92% determined by using the C_6D_6 internal standard for integration, corresponding to 9.2 turnovers.

Acknowledgment. We thank the U.S. Department of Energy, Office of Basic Energy Sciences, Division of Chemical Sciences, Geosciences and Biosciences, for supporting initial parts of the work. Current work is supported by the Center for Molecular Electrocatalysis, an Energy Frontier Research Center funded by the U.S. Department of Energy, Office of Science, Office of Basic Energy Sciences. Pacific Northwest National Laboratory is operated by Battelle for the U.S. Department of Energy.

Additional Information. Additional electrochemical details for **1-Cl**, **2-Cl**, **1-H**, **2-H**, $\text{Cp}^*\text{Ru}(\text{dmpm})\text{Cl}$ and $\text{Cp}^*\text{Ru}(\text{dmpm})\text{H}$ are provided in the supplementary material.

References

1. H. B. Gray, *Nat. Chem.*, 2009, 1, 7-7.
2. T. R. Cook, D. K. Dogutan, S. Y. Reece, Y. Surendranath, T. S. Teets and D. G. Nocera, *Chem. Rev.*, 2010, 110, 6474-6502.
3. P. M. Vignais and B. Billoud, *Chem. Rev.*, 2007, 107, 4206-4272.
4. K. A. Vincent, A. Parkin and F. A. Armstrong, *Chem. Rev.*, 2007, 107, 4366-4413.
5. A. Volbeda, M. H. Charon, C. Piras, E. C. Hatchikian, M. Frey and J. C. Fontecilla-Camps, *Nature*, 1995, 373, 580-587.

6. J. W. Peters, W. N. Lanzilotta, B. J. Lemon and L. C. Seefeldt, *Science*, 1998, 282, 1853-1858.
7. S. Shima, O. Pilak, S. Vogt, M. Schick, M. S. Stagni, W. Meyer-Klaucke, E. Warkentin, R. K. Thauer and U. Ermler, *Science*, 2008, 321, 572-575.
8. S. Ogo, K. Ichikawa, T. Kishima, T. Matsumoto, H. Nakai, K. Kusaka and T. Ohhara, *Science*, 2013, 339, 682-684.
9. T. B. Liu and M. Y. Darensbourg, *J. Am. Chem. Soc.*, 2007, 129, 7008-7009.
10. H. Li and T. B. Rauchfuss, *J. Am. Chem. Soc.*, 2002, 124, 726-727.
11. J. M. Camara and T. B. Rauchfuss, *Nat Chem*, 2011, 4, 26-30.
12. C. Tard, X. M. Liu, S. K. Ibrahim, M. Bruschi, L. De Gioia, S. C. Davies, X. Yang, L. S. Wang, G. Sawers and C. J. Pickett, *Nature*, 2005, 433, 610-613.
13. C. Tard and C. J. Pickett, *Chem. Rev.*, 2009, 109, 2245-2274.
14. B. E. Barton and T. B. Rauchfuss, *J. Am. Chem. Soc.*, 2010, 132, 14877-14885.
15. J. L. Dempsey, B. S. Brunschwig, J. R. Winkler and H. B. Gray, *Acc. Chem. Res.*, 2009, 42, 1995-2004.
16. X. Hu, B. S. Brunschwig and J. C. Peters, *J. Am. Chem. Soc.*, 2007, 129, 8988-8998.
17. V. Artero, M. Chavarot-Kerlidou and M. Fontecave, *Angew. Chem. Int. Ed.*, 2011, 50, 7238-7266.
18. S. Ott, M. Kritikos, B. Akermark, L. C. Sun and R. Lomoth, *Angew. Chem. Int. Ed.*, 2004, 43, 1006-1009.
19. W. M. Singh, T. Baine, S. Kudo, S. Tian, X. A. N. Ma, H. Zhou, N. J. DeYonker, T. C. Pham, J. C. Bollinger, D. L. Baker, B. Yan, C. E. Webster and X. Zhao, *Angew. Chem. Int. Ed.*, 2012, 51, 5941-5944.
20. H. I. Karunadasa, C. J. Chang and J. R. Long, *Nature*, 2010, 464, 1329-1333.
21. V. S. Thoi, Y. Sun, J. R. Long and C. J. Chang, *Chem. Soc. Rev.*, 2013, 42, 2388-2400.
22. G. Berggren, A. Adamska, C. Lambertz, T. R. Simmons, J. Esselborn, M. Atta, S. Gambarelli, J. M. Mouesca, E. Reijerse, W. Lubitz, T. Happe, V. Artero and M. Fontecave, *Nature*, 2013, 499, 66-69.
23. J. C. Fontecilla-Camps, A. Volbeda, C. Cavazza and Y. Nicolet, *Chem. Rev.*, 2007, 107, 4273-4303.
24. W. Lubitz, E. Reijerse and M. van Gastel, *Chem. Rev.*, 2007, 107, 4331-4365.
25. J. M. Camara and T. B. Rauchfuss, *Nat Chem*, 2012, 4, 26-30.
26. M. Rakowski DuBois and D. L. DuBois, *Chem. Soc. Rev.*, 2009, 38, 62-72.
27. M. Rakowski Dubois and D. L. Dubois, *Acc. Chem. Res.*, 2009, 42, 1974-1982.
28. D. L. DuBois and R. M. Bullock, *Eur. J. Inorg. Chem.*, 2011, 2011, 1017-1027.
29. R. M. Bullock, A. M. Appel and M. L. Helm, *Chem. Commun.*, 2014, 50, 3125-3143.
30. A. D. Wilson, R. H. Newell, M. J. McNevin, J. T. Muckerman, M. Rakowski DuBois and D. L. DuBois, *J. Am. Chem. Soc.*, 2006, 128, 358-366.
31. M. L. Helm, M. P. Stewart, R. M. Bullock, M. R. DuBois and D. L. DuBois, *Science*, 2011, 333, 863-866.
32. A. D. Wilson, R. K. Shoemaker, A. Miedaner, J. T. Muckerman, D. L. DuBois and M. Rakowski DuBois, *Proc. Natl. Acad. Sci. U.S.A.*, 2007, 104, 6951-6956.
33. E. I. Musina, V. V. Khrizanforova, I. D. Strel'nik, M. I. Valitov, Y. S. Spiridonova, D. B. Krivolapov, I. A. Litvinov, M. K. Kadirov, P. Lönnecke, E. Hey-Hawkins, Y. H. Budnikova, A. A. Karasik and O. G. Sinyashin, *Chem. Eur. J.*, 2014, 20, 3169-3182.

34. G. M. Jacobsen, J. Y. Yang, B. Twamley, A. D. Wilson, R. M. Bullock, M. Rakowski DuBois and D. L. DuBois, *Energy Environ. Sci.*, 2008, 1, 167-174.
35. E. S. Wiedner, J. Y. Yang, W. G. Dougherty, W. S. Kassel, R. M. Bullock, M. R. DuBois and D. L. DuBois, *Organometallics*, 2010, 29, 5390-5401.
36. C. S. Seu, D. Ung, M. D. Doud, C. E. Moore, A. L. Rheingold and C. P. Kubiak, *Organometallics*, 2013, 32, 4556-4563.
37. E. S. Wiedner and M. L. Helm, *Organometallics*, 2014, DOI: 10.1021/om4010669, in press, DOI: 10.1021/om4010669.
38. S. Lense, M.-H. Ho, S. Chen, A. Jain, S. Raugei, J. C. Linehan, J. A. S. Roberts, A. M. Appel and W. Shaw, *Organometallics*, 2012, 31, 6719-6731.
39. A. Dutta, S. Lense, J. Hou, M. H. Engelhard, J. A. S. Roberts and W. J. Shaw, *J. Am. Chem. Soc.*, 2013, 135, 18490-18496.
40. J. Y. Yang, R. M. Bullock, W. J. Shaw, B. Twamley, K. Frazee, M. R. DuBois and D. L. DuBois, *J. Am. Chem. Soc.*, 2009, 131, 5935-5945.
41. J. Y. Yang, S. Chen, W. G. Dougherty, W. S. Kassel, R. M. Bullock, D. L. DuBois, S. Raugei, R. Rousseau, M. Dupuis and M. Rakowski DuBois, *Chem. Commun.*, 2010, 46, 8618-8620.
42. J. Y. Yang, S. E. Smith, T. Liu, W. G. Dougherty, W. A. Hoffert, W. S. Kassel, M. R. DuBois, D. L. DuBois and R. M. Bullock, *J. Am. Chem. Soc.*, 2013, 135, 9700-9712.
43. S. E. Smith, J. Y. Yang, D. L. DuBois and R. M. Bullock, *Angew. Chem. Int. Ed.*, 2012, 51, 3152-3155.
44. P. Das, M.-H. Ho, M. O'Hagan, W. J. Shaw, R. Morris Bullock, S. Raugei and M. L. Helm, *Dalton Trans.*, 2014, 43, 2744-2754.
45. T. Liu, S. Chen, M. J. O'Hagan, M. Rakowski DuBois, R. M. Bullock and D. L. DuBois, *J. Am. Chem. Soc.*, 2012, 134, 6257-6272.
46. T. Liu, D. L. DuBois and R. M. Bullock, *Nat. Chem.*, 2013, 5, 228-233.
47. T. Liu, X. Wang, C. Hoffmann, D. L. DuBois and R. M. Bullock, *Angew. Chem. Int. Ed.*, 2014, DOI: 10.1002/anie.201105266, DOI: 10.1002/anie.201402090.
48. J. M. Darmon, S. Raugei, T. Liu, E. B. Hulley, C. J. Weiss, R. M. Bullock and M. L. Helm, *ACS Catalysis*, 2014, 4, 1246-1260.
49. D. M. Heinekey and W. J. Oldham, *Chem. Rev.*, 1993, 93, 913-926.
50. P. G. Jessop and R. H. Morris, *Coord. Chem. Rev.*, 1992, 121, 155-284.
51. M. S. Chinn and D. M. Heinekey, *J. Am. Chem. Soc.*, 1990, 112, 5166-5175.
52. J. K. Law, H. Mellows and D. M. Heinekey, *J. Am. Chem. Soc.*, 2002, 124, 1024-1030.
53. M. Jimenez-Tenorio, M. C. Puerta and P. Valerga, *Inorg. Chem.*, 1994, 33, 3515-3520.
54. I. de los Ríos, M. Jiménez Tenorio, J. Padilla, M. C. Puerta and P. Valerga, *Organometallics*, 1996, 15, 4565-4574.
55. F. A. Jalón, B. R. Manzano, A. Caballero, M. C. Carrión, L. Santos, G. Espino and M. Moreno, *J. Am. Chem. Soc.*, 2005, 127, 15364-15365.
56. T. A. Tronic, M. Rakowski DuBois, W. Kaminsky, M. K. Coggins, T. Liu and J. M. Mayer, *Angew. Chem. Int. Ed.*, 2011, 50, 10936-10939.
57. T. A. Tronic, W. Kaminsky, M. K. Coggins and J. M. Mayer, *Inorg. Chem.*, 2012, 51, 10916-10928.
58. M. Rakowski DuBois and D. L. DuBois, *Comptes Rendus Chimie*, 2008, 11, 805-817.
59. N. Wang, M. Wang, Y. Wang, D. Zheng, H. Han, M. S. G. Ahlquist and L. Sun, *J. Am. Chem. Soc.*, 2013, 135, 13688-13691.

60. T. A. Luther and D. M. Heinekey, *Inorg. Chem.*, 1998, 37, 127-132.
61. R. Gelabert, M. Moreno, J. M. Lluch, A. Lledós, V. Pons and D. M. Heinekey, *J. Am. Chem. Soc.*, 2004, 126, 8813-8822.
62. S. Gründemann, H.-H. Limbach, G. Buntkowsky, S. Sabo-Etienne and B. Chaudret, *The Journal of Physical Chemistry A*, 1999, 103, 4752-4754.
63. P. A. Maltby, M. Schlaf, M. Steinbeck, A. J. Lough, R. H. Morris, W. T. Klooster, T. F. Koetzle and R. C. Srivastava, *J. Am. Chem. Soc.*, 1996, 118, 5396-5407.
64. E. S. Wiedner, J. Y. Yang, S. Chen, S. Raugai, W. G. Dougherty, W. S. Kassel, M. L. Helm, R. M. Bullock, M. Rakowski DuBois and D. L. DuBois, *Organometallics*, 2011, 31, 144-156.
65. I. Kaljurand, A. Kutt, L. Soovali, T. Rodima, V. Maemets, I. Leito and I. A. Koppel, *J. Org. Chem.*, 2005, 70, 1019-1028.
66. R. S. Nicholson and I. Shain, *Anal. Chem.*, 1964, 36, 706-723.
67. J. M. Saveant and E. Vianello, *Electrochim. Acta*, 1965, 10, 905-920.
68. J. M. Savéant and E. Vianello, *Electrochim. Acta*, 1967, 12, 629-646.
69. T. Richardson, S. de Gala, R. H. Crabtree and P. E. M. Siegbahn, *J. Am. Chem. Soc.*, 1995, 117, 12875-12876.
70. R. Custelcean and J. E. Jackson, *Chem. Rev.*, 2001, 101, 1963-1980.
71. J. P. Collman, P. S. Wagenknecht, J. E. Hutchison, N. S. Lewis, M. A. Lopez, R. Guilard, M. L'Her, A. A. Bothner-By and P. K. Mishra, *J. Am. Chem. Soc.*, 1992, 114, 5654-5664.
72. T. Matsumoto, K. Kim and S. Ogo, *Angew. Chem. Int. Ed.*, 2011, 50, 11202-11205.
73. A. Svetlanova-Larsen, C. R. Zoch and J. L. Hubbard, *Organometallics*, 1996, 15, 3076-3087.
74. A. Tahiri, V. Guerchais, L. Toupet and C. Lapinte, *J. Organomet. Chem.*, 1990, 381, C47-C51.
75. G. J. Kubas, C. J. Burns, G. R. K. Khalsa, L. S. Van Der Sluys, G. Kiss and C. D. Hoff, *Organometallics*, 1992, 11, 3390-3404.
76. J. C. Gordon and G. J. Kubas, *Organometallics*, 2010, 29, 4682-4701.
77. L. Luo and S. P. Nolan, *Organometallics*, 1994, 13, 4781-4786.
78. W. Lin, S. R. Wilson and G. S. Girolami, *Organometallics*, 1997, 16, 2356-2361.

Supplementary Information for

**Electrochemical Oxidation of H₂ Catalyzed by Ruthenium Hydride Complexes Bearing P₂N₂
Ligands With Pendant Amines as Proton Relays**

Tianbiao Liu,* Mary Rakowski DuBois, Daniel L. DuBois and R. Morris Bullock*

Center for Molecular Electrocatalysis, Physical Sciences Division, Pacific Northwest National
Laboratory, P.O. Box 999, K2-57, Richland, WA 99352

morris.bullock@pnl.gov, tianbiao.liu@pnl.gov

Contents

Figure S1. Cyclic voltammograms of 1-Cl recorded at various scan rates.....	2
Figure S2. Cyclic voltammograms of 2-Cl recorded at various scan rates.....	3
Figure S3. Cyclic voltammograms of 1-H recorded at various scan rates.....	4
Figure S4. Cyclic voltammograms of 2-H recorded at various scan rates.....	4
Figure S5. Plots of i_{cat}/i_p versus DBU base concentration for 1-H and 2-H.....	5
Figure S6. Electrochemical H ₂ oxidation by 1-H before and after saturation of the solution with H ₂ O (adding 20 μL H ₂ O into 1.0 mL PhF solution).....	5
Figure S7. Cyclic voltammograms of Cp*Ru(dmpm)Cl.....	6
Figure S8. Cyclic voltammograms of Cp*Ru(dmpm)Cl.....	7
Figure S9. Cyclic voltammograms of Cp*Ru(dmpm)H.....	7
Figure S10. Attempted electrochemical H ₂ oxidation by Cp*Ru(dmpm)H	8
Figure S11. Electrochemical H ₂ oxidation by 2-H	9
Calculation of thermodynamic equilibrium potential of [DBU-H] ⁺ /DBU for H ₂ oxidation.....	10
Overpotential (η) calculations for 1-H and 2-H.	10

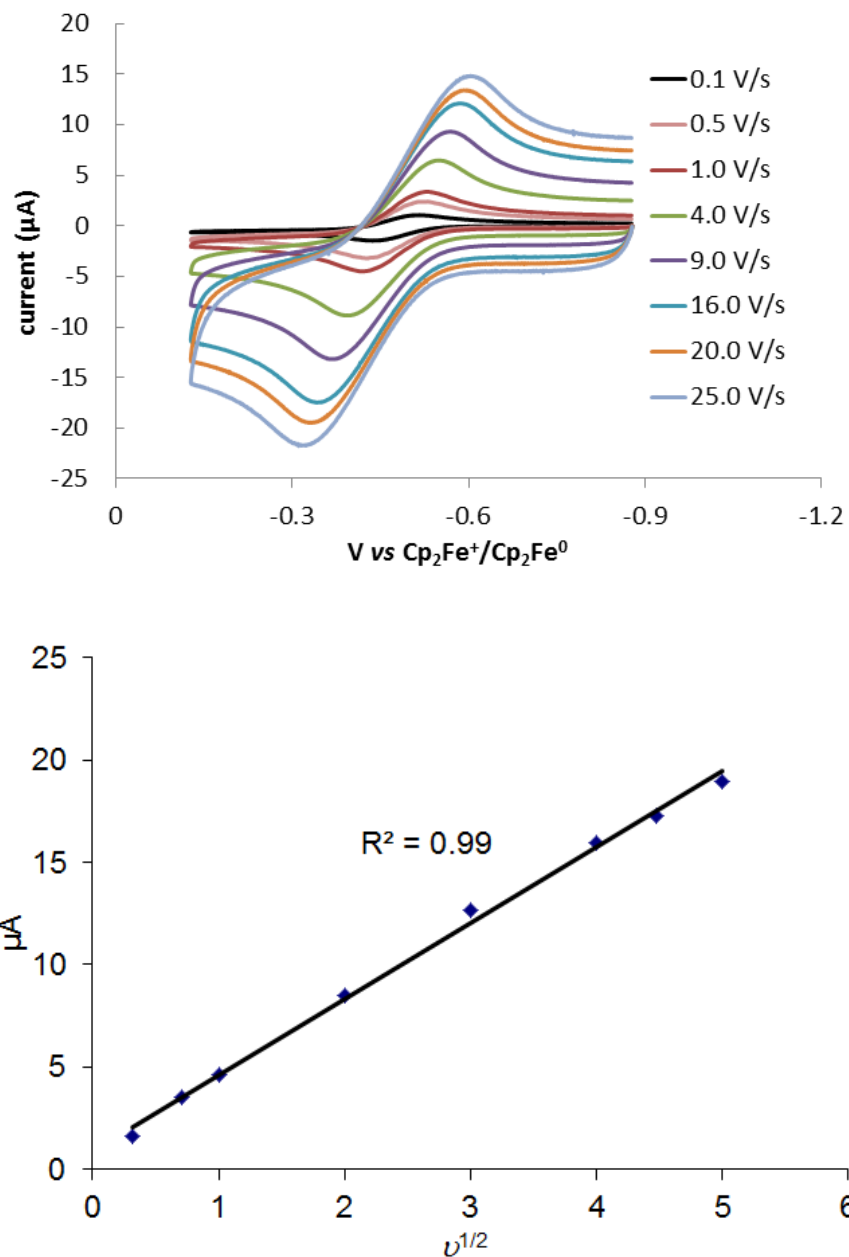


Figure S1. Cyclic voltammograms of **1-Cl** recorded at various scan rates (top), 0.1 - 25 V/s; electrolyte, 0.1 M ⁿBu₄NB(C₆F₅)₄ in PhF; under Ar (1.0 atm). Plot of *i*_a versus the root of scan rate (bottom). A linear plot indicates the electrochemical process is under diffusion control.

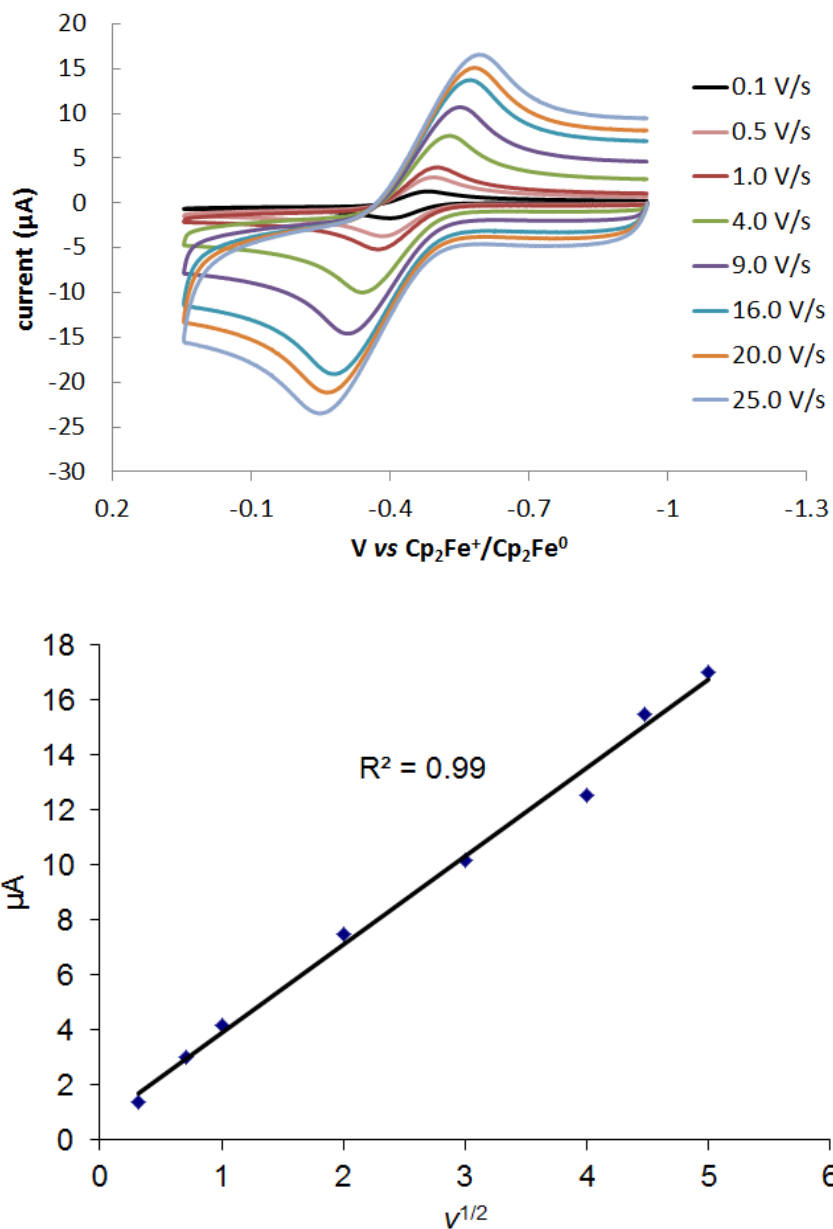


Figure S2. Cyclic voltammograms of **2-Cl** recorded at various scan rates (top), 0.1 - 25 V/s; electrolyte, 0.1 M ⁿBu₄NB(C₆F₅)₄ in PhF; under Ar (1.0 atm). Plot of *i*_a versus the root of scan rate (bottom). A linear plot indicates the electrochemical process is under diffusion control.

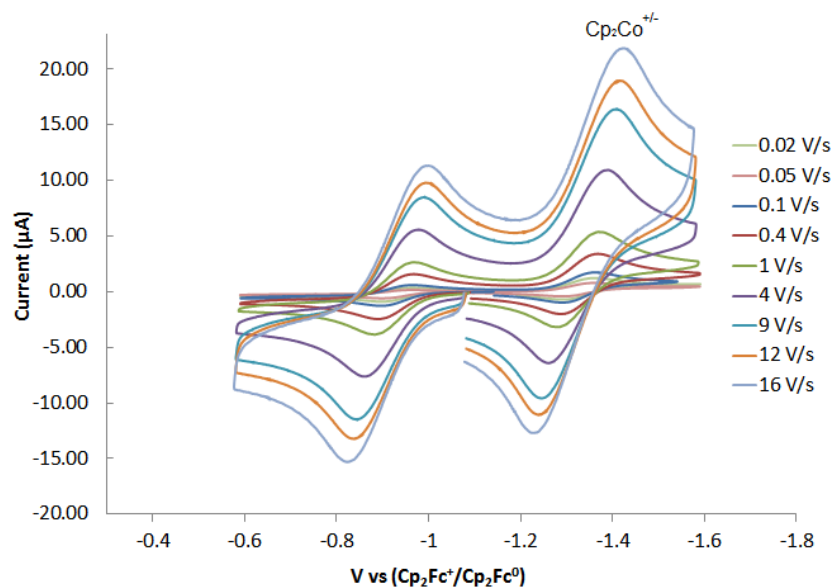


Figure S3. Cyclic voltammograms of **1-H** recorded at various scan rates (top), 0.1 - 16 V/s; electrolyte, 0.1 M ⁿBu₄NB(C₆F₅)₄ in PhF; under Ar (1.0 atm); Cp₂CoPF₆ (-1.33 V) as internal reference.

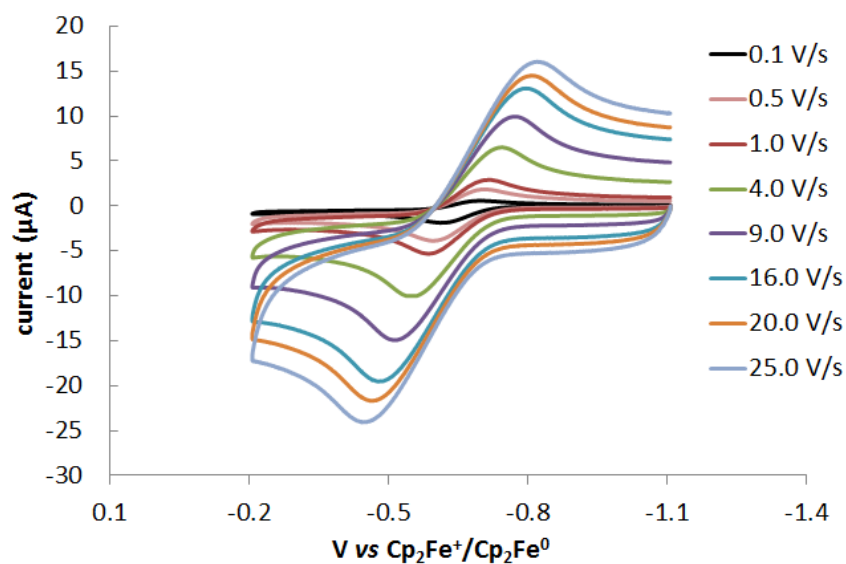


Figure S4. Cyclic voltammograms of **2-H** recorded at various scan rates (top), 0.1 - 16 V/s; electrolyte, 0.1 M ⁿBu₄NB(C₆F₅)₄ in PhF; under Ar (1.0 atm).

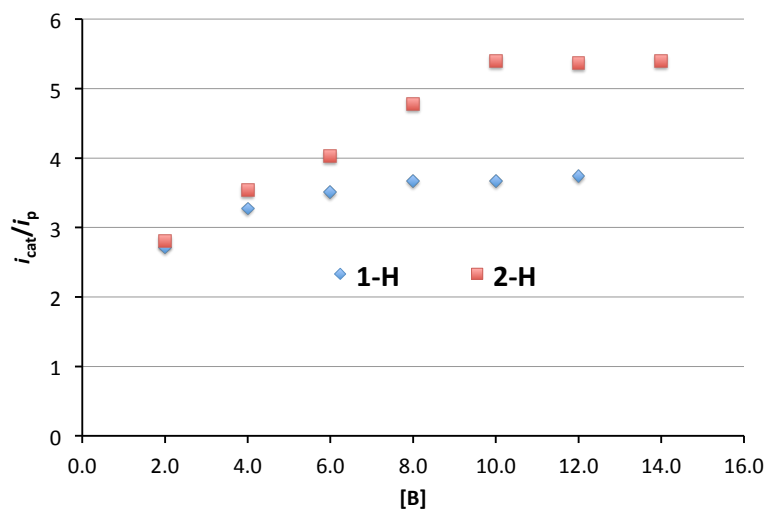


Figure S5. Plots of i_{cat}/i_p versus DBU base concentration for **1-H** and **2-H**. Conditions: 1.0 mM solution of **1-H** or **2-H** in PhF at 22 °C under 1.0 atm H₂ at 20 mV/s scan.

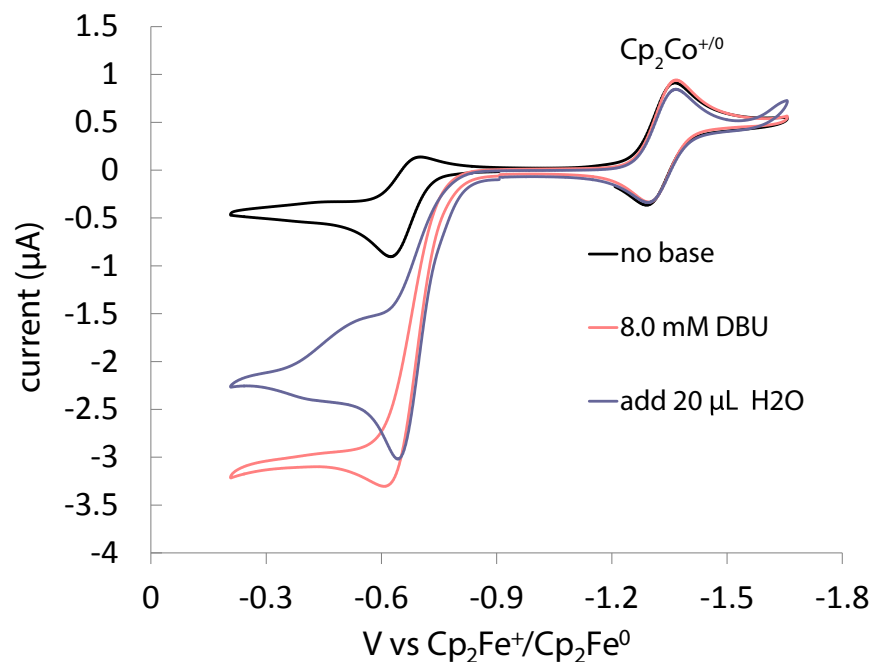


Figure S6. Electrochemical H₂ oxidation by **1-H** before and after saturation of the solution with H₂O (adding 20 µL H₂O into 1.0 mL PhF solution). Conditions: 1.0 mM **1-H**; 0.1 M ⁿBu₄NB(C₆F₅)₄; 1.0 atm H₂; scan rate, 20 mV/s; 22 °C; Cp₂CoPF₆ (-1.33 V) as internal reference.

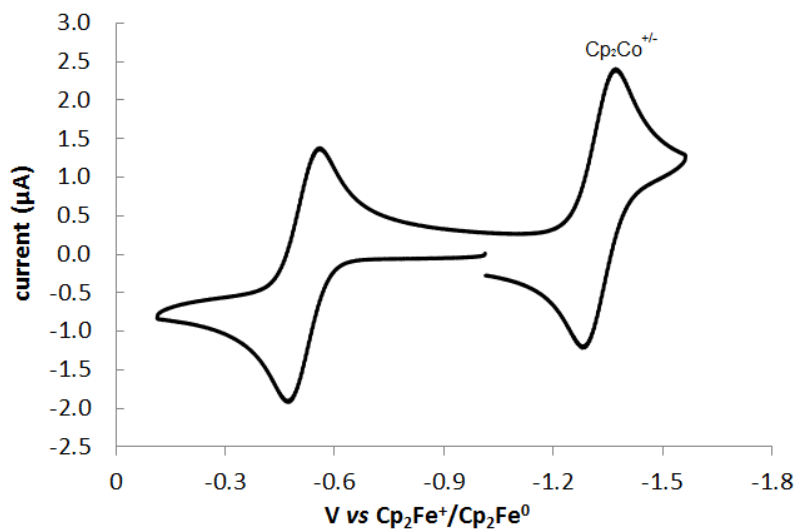
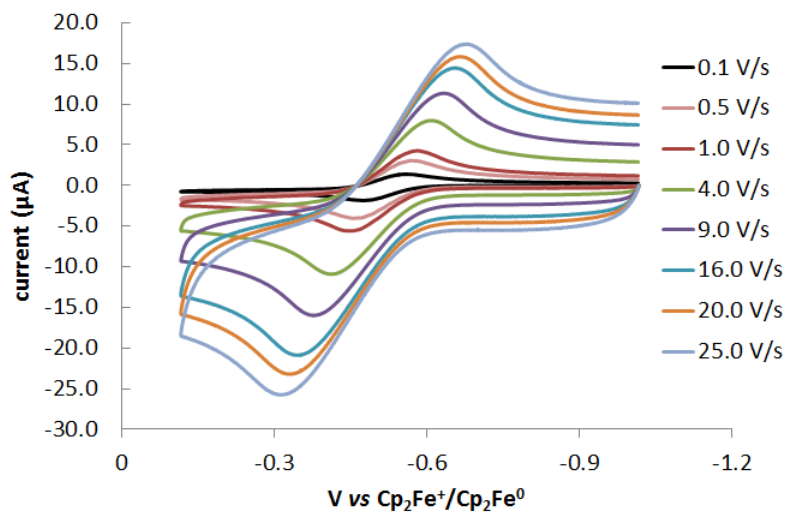


Figure S7. Cyclic voltammograms of Cp^{*}Ru(dmpm)Cl. Conditions: 1.0 mM; 0.1 M ⁿBu₄NB(C₆F₅)₄; under 1.0 atm Ar; scan rate, 100 mV/s; Cp₂CoPF₆ (-1.33 V) as internal reference.



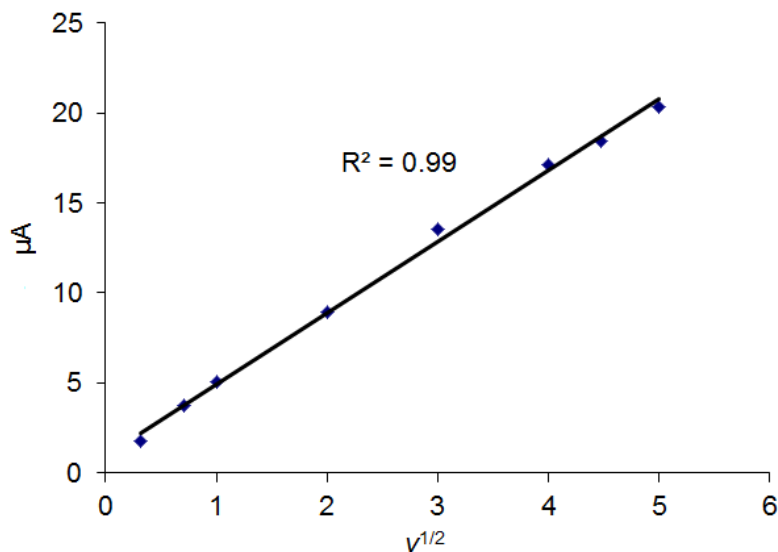


Figure S8. Cyclic voltammograms of Cp*Ru(dmpm)Cl recorded at various scan rates (top), 0.1 - 25 V/s; electrolyte, 0.1 M $n\text{Bu}_4\text{NB}(\text{C}_6\text{F}_5)_4$ in PhF; under Ar (1.0 atm). Plot of i_a versus the root of scan rate (bottom). A linear plot indicates the electrochemical process is under diffusion control.

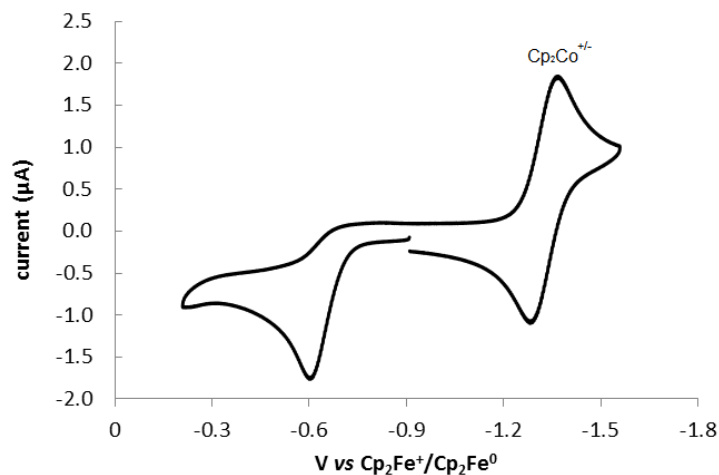


Figure S9. Cyclic voltammograms of Cp*Ru(dmpm)H recorded at various scan rates (top), 0.1 - 25 V/s; electrolyte, 0.1 M $n\text{Bu}_4\text{NB}(\text{C}_6\text{F}_5)_4$ in PhF; Cp_2CoPF_6 (-1.33 V) as internal reference; under Ar (1.0 atm).

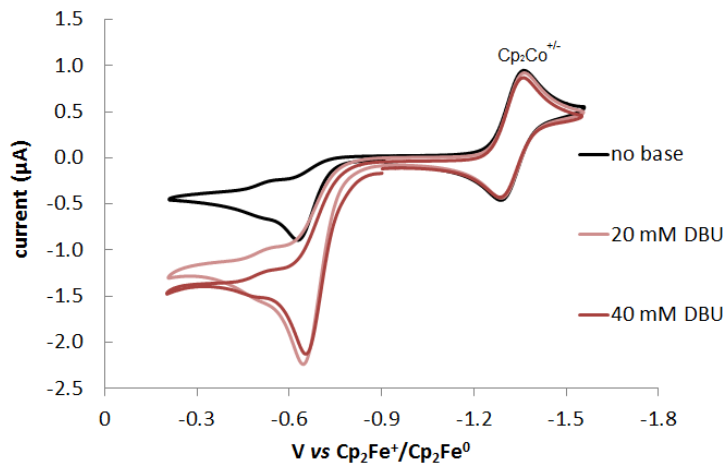
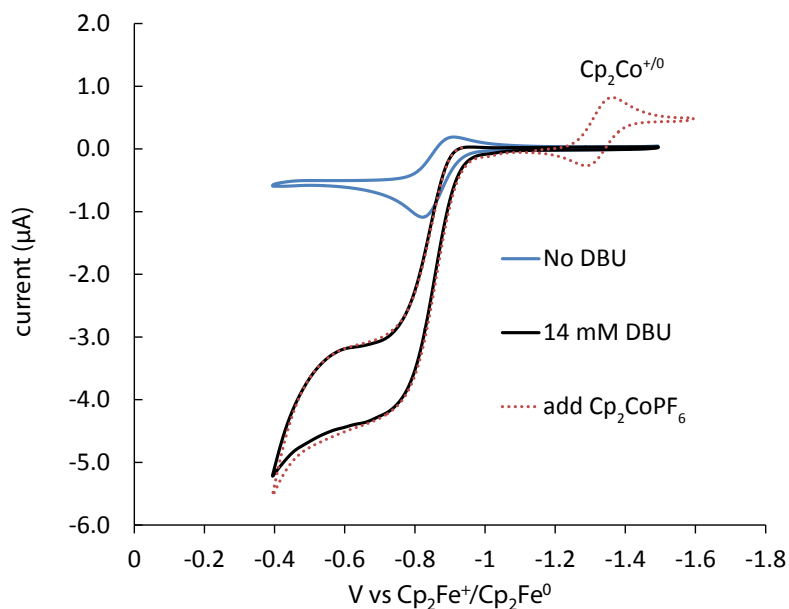


Figure S10. Attempted electrochemical H₂ oxidation by Cp^{*}Ru(dmpm)H under 1.0 atm H₂ with increasing concentrations of DBU as indicated in the legend. Conditions: 1.0 mM analyt of Ru-complexes; 0.1 M ⁿBu₄NB(C₆F₅)₄; 1.0 atm H₂; scan rate, 20 mV/s; 22 °C; Cp₂CoPF₆ (-1.33 V) as internal reference.



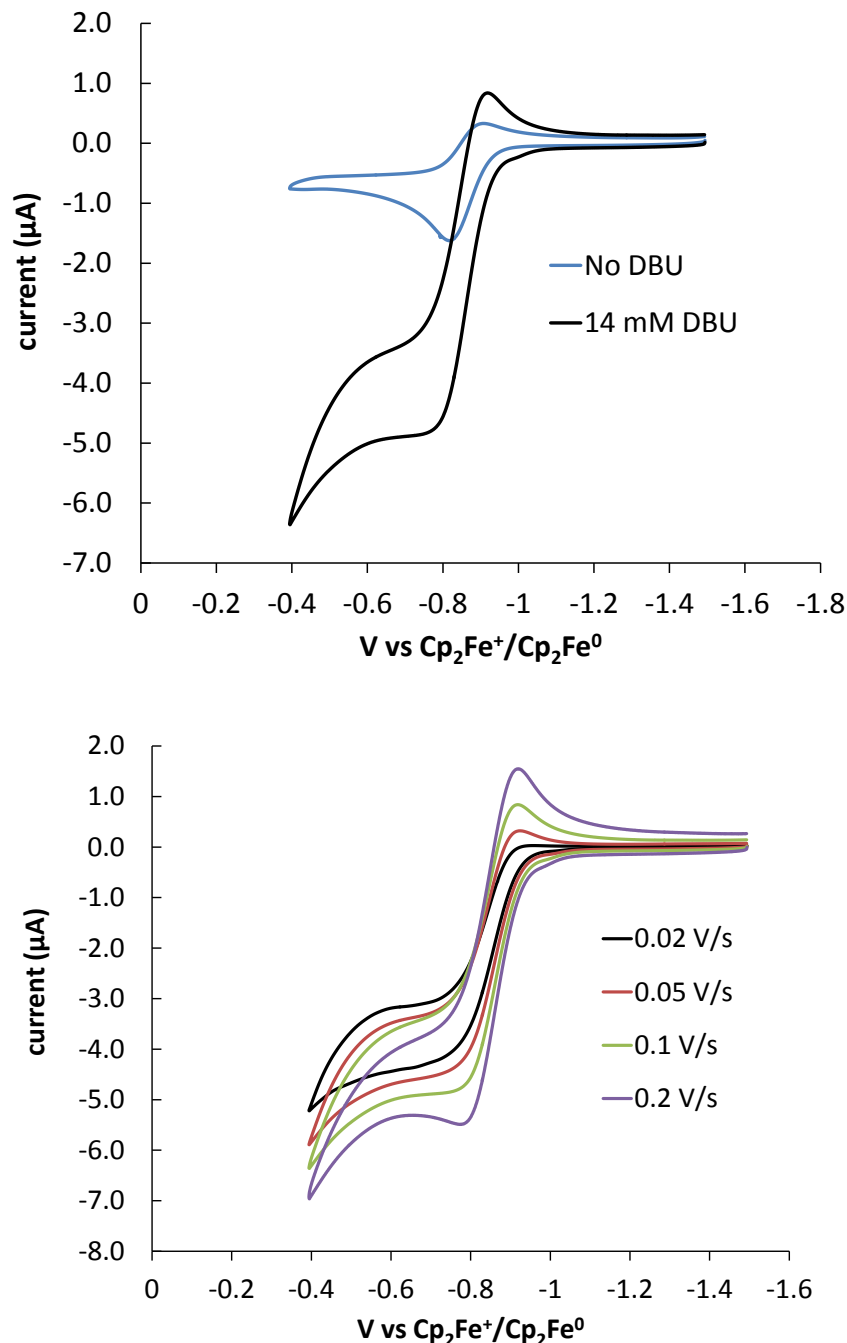


Figure S11. Electrochemical H₂ oxidation by **2-H** under 1.0 atm H₂ in the presence of 14 mM DBU. (top) Cyclic voltammograms recorded at 0.02 V/s: the overlapped catalytic waves (black trace and red dot trace) confirmed the presence of the internal reference, Cp₂CoPF₆ (-1.33 V), has no influence on the catalytic current for the oxidation of H₂. (middle) Cyclic voltammograms recorded at 0.1 V/s. (bottom) Cyclic voltammograms for the oxidation of H₂ by **2-H** recorded at 0.02 V/s, 0.05 V/s, 0.1 V/s and 0.2 V/s for a same solution under catalytic conditions (1.0 atm H₂

in the presence of 14 mM DBU). Conditions: 1.0 mM **2-H**; 0.1 M $n\text{Bu}_4\text{NB}(\text{C}_6\text{F}_5)_4$; 1.0 atm H_2 ; scan rate, 20 mV/s; 22 °C; Cp_2CoPF_6 (-1.33 V) as internal reference.

Calculation of thermodynamic equilibrium potential of $[\text{DBU-H}]^+/\text{DBU}$ for H_2 oxidation.

The poor solubility of $[\text{DBU-H}]^+$ precludes direct experimental measurement of the thermodynamic equilibrium potential by the open circuit potential method developed by our group.¹⁻³ Therefore, the thermodynamic equilibrium potential of $[\text{DBU-H}]^+/\text{DBU}$ was estimated.² The relationship of thermodynamic equilibrium potential for different $[\text{B-H}]^+/\text{B}$ can be expressed as equation S2.

$$E^\circ_{([\text{B-H}]^+/\text{B})} = E^\circ_{\text{H}^+} - \left(\frac{2.303RT}{F}\right) pK_{a,([\text{B-H}]^+)} \quad (\text{equation S1})$$

$$E^\circ_{([\text{B}'-H]^+/\text{B}')} = E^\circ_{([\text{B-H}]^+/\text{B})} - \left(\frac{2.303RT}{F}\right) \Delta pK_a \quad (\text{equation S2})$$

Since $E^\circ_{([\text{Et}_3\text{N-H}]^+/\text{Et}_3\text{N})}$ in PhF was determined as -1.01 V vs $\text{Cp}_2\text{Fe}^{+/0}$, $E^\circ_{([\text{DBU-H}]^+/\text{DBU})}$ in PhF can be calculated using ΔpK_a ($[\text{DBU-H}]^+ - [\text{Et}_3\text{N-H}]^+$), 5.52, in CH_3CN :

$$\begin{aligned} & E^\circ_{([\text{DBU-H}]^+/\text{DBU})} \\ &= E^\circ_{([\text{Et}_3\text{N-H}]^+/\text{Et}_3\text{N})} - \left(\frac{2.303RT}{F}\right) \Delta pK_a = -1.31 \text{ V} \end{aligned}$$

Overpotential (η) calculations for **1-H** and **2-H**.

$$\eta = \text{Operating potential} - E^\circ_{([\text{DBU-H}]^+/\text{DBU})} \quad (\text{equation S3})$$

The operating potential is defined as the middle point of the catalytic wave for the H_2 oxidation, -0.82 V and -0.85 vs $\text{Cp}_2\text{Fe}^{+/0}$ for **1-H** and **2-H** respectively.

For **1-H**,

$$\eta(\text{DBU}) = -0.71 - (-1.31) = 0.60 \text{ V}$$

For **2-H**,

$$\eta(\text{DBU}) = -0.85 - (-1.31) = 0.46 \text{ V}$$

References

- (1) Pool, D. H.; Stewart, M. P.; O'Hagan, M.; Shaw, W. J.; Roberts, J. A. S.; Bullock, R. M.; DuBois, D. L. *Proc. Natl. Acad. Sci. U. S. A.* **2012**, *109*, 15634-15639.
- (2) Liu, T.; DuBois, D. L.; Bullock, R. M. *Nat. Chem.* **2013**, *5*, 228-233.
- (3) Roberts, J. A. S.; Bullock, R. M. *Inorg. Chem.* **2013**, *52*, 3823-3835.